Life Sciences 300 (2022) 120593

Contents lists available at ScienceDirect

Life Sciences

journal homepage: www.elsevier.com/locate/lifescie

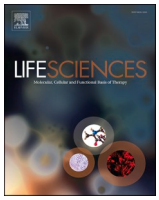

Review article

Recent progress in the early detection of cancer based on CD44 biomarker; nano-biosensing approaches

Youkabed Kazemi [a,b,1], Sadegh Dehghani [a,1], Rahim Nosrati [c], Seyed Mohammad Taghdisi [d], Khalil Abnous [a,e], Mona Alibolandi [a,b,*], Mohammad Ramezani [a,b,*]

[a] Pharmaceutical Research Center, Pharmaceutical Technology Institute, Mashhad University of Medical Sciences, Mashhad, Iran
[b] Department of Pharmaceutical Biotechnology, School of Pharmacy, Mashhad University of Medical Sciences, Mashhad, Iran
[c] Cellular and Molecular Research Center, School of Medicine, Guilan University of Medical Sciences, Rasht, Iran
[d] Targeted Drug Delivery Research Center, Pharmaceutical Technology Institute, Mashhad University of Medical Sciences, Mashhad, Iran
[e] Department of Medicinal Chemistry, School of Pharmacy, Mashhad University of Medical Sciences, Mashhad, Iran

ARTICLE INFO

Keywords:
CD44
Cancer biomarker
Biosensor
Nanosensor
Aptasensor

ABSTRACT

CD44 is a cell matrix adhesion molecule overexpressed on the cell surfaces of the major cancers. CD44 as a cancer-related biomarker has an essential role in the invasion and metastasis of cancer. The detection and quantification of CD44 can provide essential information useful for clinical cancer diagnosis. In this regard, biosensors with sensitive and specific properties, give prominence to the development of CD44 detection platforms. To date, various aptamer-based sensitive-enhancers together with nanoparticles (NPs) have been combined into the biosensors systems to provide an innovative biosensing method (aptasensors/nano-aptasensors) with substantially improved detection limit. This review article discusses the recent advances in the field of biosensors, nanobiosensors, and aptasensors for the quantitative determination of CD44 and the detection of CD44-expressing cancer cells.

1. Introduction

Cancer is the second most extensive disease with a rapidly growing mortality rate worldwide over the past decades [1,2]. Nowadays, the detection of cancer-specific biomarkers has attracted considerable interest for early stage diagnosis and clinical management of a wide range of cancers [3,4].

CD44 is an extracellular cell matrix adhesion molecule belonging to the transmembrane glycoproteins known to be overexpressed on the surfaces of several cancers, comprising breast and lung cancers, and thus can be frequently employed as a cancer-targeting biomarker for the cancer diagnosis and treatment [5]. CD44 may exist as either standard (CD44s) or variant (CD44v) isoforms (Fig. 1) [6]. It has crucial roles in cellular events such as adhesion, aggregation, migration, and signal transduction [7]. CD44 receptor is associated with tumor invasion, prognosis, progression, and metastasis. It has been also associated with tumor development and progression, and provided many prospects for targeting delivery of therapeutics for cancer therapy [7–9]. CD44 is known as one of the most popular biomarkers of cancer stem cells (CSCs) of various origins especially breast, colon, and pancreas making this receptor an ideal target for the delivery of diagnostic and therapeutic agents [1,10,11]. CD44 was able to interact with a number of extracellular components, including hyaluronic acid (HA/hyaluronan) [5].

HA, the main part of the extracellular matrix (ECM), is a natural glycosaminoglycans (GAGs) or mucopolysaccharide containing alternate repeat of *N*-acetyl-D-glucosamine and D-glucuronic acid. HA is involved in cell growth and structural stability of tissue. It has drawn lots of attention in biomedicine, especially for the targeted drug delivery due to it non-toxic, non-immunogenic, biocompatible, biodegradable, and hydrophilic properties [7]. There are numerous HA receptors overexpressed on tumor cells surfaces. Cluster of differentiation 44 (CD44), the receptor for HA-mediated motility (RHAMM) and lymphatic vessel endocytic receptor (LYVE-1) are the common HA receptors. Among these, CD44 has a key role in the specific interactions with HA present on cancer cells surfaces and has been extensively explored [7].

The common methods used for the detection of CD44 including

* Corresponding authors at: School of Pharmacy, Pharmaceutical Research Center, Mashhad University of Medical Sciences, , P.O. Box: 91775-1365, Mashhad, Iran.
E-mail addresses: alibolandim@mums.ac.ir (M. Alibolandi), ramezanim@mums.ac.ir (M. Ramezani).
[1] These authors contributed equally

https://doi.org/10.1016/j.lfs.2022.120593
Received 6 March 2022; Received in revised form 24 April 2022; Accepted 26 April 2022
Available online 29 April 2022

immunohistochemistry, PCR and enzyme-linked immunosorbent assay (ELISA), despite having good sensitivity and specificity, are time-consuming, have a low shelf-life and need expensive instruments, thus limiting their use for patients' care and usually are for research use only [13–15]. Therefore, it would be important to develop new techniques for specific and sensitive determination of CD44 in the various cancers without encountering the restriction imposed by the above-mentioned methods. Among new approaches developed for the CD44 detection, biosensing methods are practical alternatives for laboratory tests owing to their quickness, lower limit of detection (LOD), simplicity, sensitivity, being real-time, effective and high quality outcomes [1,16].

Biosensors are powerful analytical tools using a biological recognition element coupled to a transducer capable of quantitative detection of analytes [17]. Nanomaterials (NMs)/nanoparticles (NPs) have attracted great interest in the construction of biosensors with improved performance. These biosensors are called nanobiosensors which can provide more sensitive, robust, and reliable platforms for biomarkers detection and offer hopeful capacities for nanomedicine [18,19]. There are numerous forms of physicochemical transducers including electrochemical, optical, piezoelectric, thermometric, and micromechanical-based platforms.

In this review, the recent progress in various types of biosensing approaches for the determination of CD44 as a biomarker of cancer, their designs, and their working principles are discussed. Moreover, we provided a brief outline of the NPs-based biosensors and aptasensors for the development of biosensing assays for CD44 detection.

2. Optical-based biosensors for CD44 detection

Optical biosensors are the most accessible biosensors which have found various applications in biomedicine and pharmaceutics [17,20]. In optical biosensors, a signal is produced based on the optical properties of waveguide in proportion to the concentration of the analyte [20] and they had made rapid advances for real-time, label-free and parallel detection of various materials [17]. In this section, we have summarized the reported optical biosensors/nano-biosensors for CD44 detection. Tables 1 and 2 display the prominent examples of optical-based CD44 biosensors.

2.1. Luminescence-based CD44 biosensors

Luminescence can be described as a phenomenon of producing a light emission from other sources of energy except heat [17,21]. It can be categorized into diverse kinds of light-emitting processes depending upon source of energy. For instance, the chemical and electrochemical reactions are the source of light in chemiluminescence (CL) and electrochemiluminescence (ECL), respectively [22]. Luminescence-based biosensors have been emerged as high selectivity, sensitivity, and large linear quantitative range methods, and have a remarkable performance in the lab-on-chip approaches [23,24]. Several luminescence-based biosensors have been designed for the detection of CD44 (Table 1).

A quantum dot (QD)-labeled near-field optical microscopy (NSOM) probe was used to demonstrate the localization of CD44 on mesenchymal stem cells (MSCs). Taking advantage of QD luminance (fluorescence), they clearly enhanced the signal-to-noise (S/N) ratio as well as the reproducibility of NSOM probe [25]. As they can be optimized in the context of biocompatibility, sizes, charges, stability, surface coating, and core/shell structure, QDs are being investigated for the construction of the biosensing platforms. The size of QDs is one of the most essential features, as it determines their optical quality as well as their range of interactions with colloidal media [26]. The use of QDs in biosensing systems is limited by their toxicity, intrinsic blinking, chemical instability, and poor fluorescence [27,28].

Qiu and co-workers fabricated a novel single-cell approach using solid-state zinc-coadsorbed carbon-QD (ZnCQDs) nanocomposites as an ECL probe together with substrates including graphene oxide (GO)/gold nanoparticles (AuNPs) for the identification of CD44-positive breast

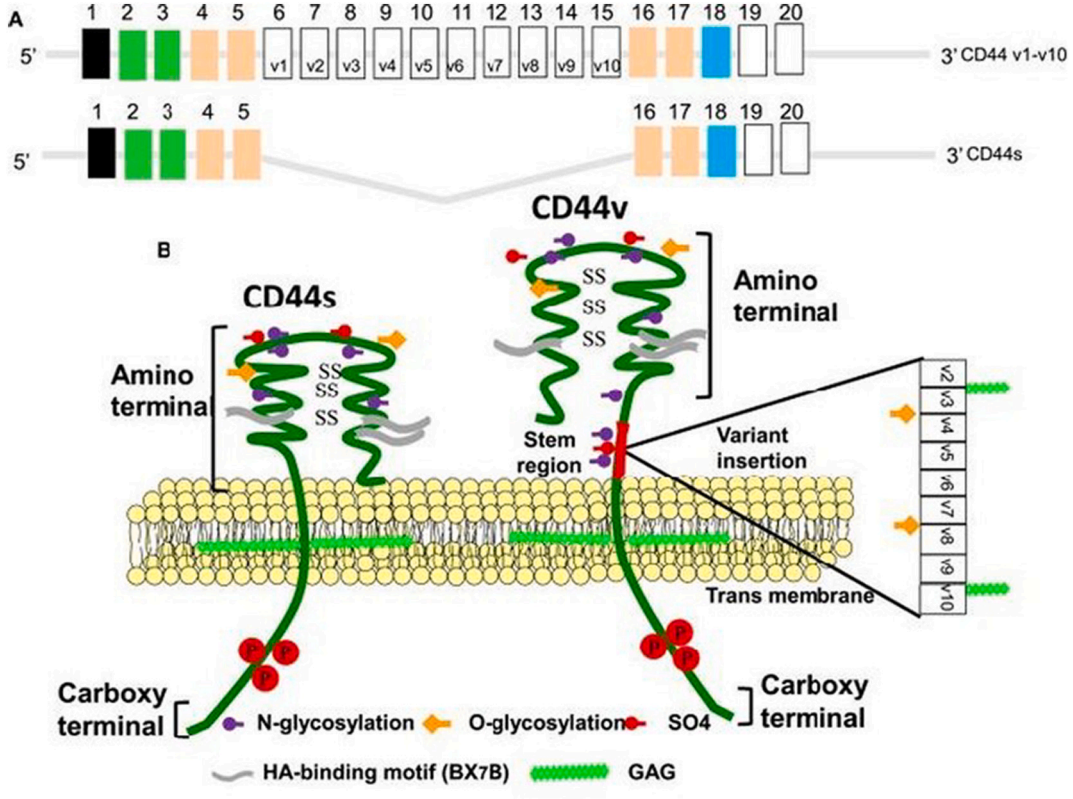

Fig. 1. The gene and morphological structure of CD44 isoforms. Reprinted with permission from [12].

Table 1
The summery of the described luminescence and fluorescence biosensors and nano-biosensors for CD44 detection.

Detection method	Strategy	Recognition unit	Target/Cell	Sample	LOD	LR	Ref.
Luminescence	HA-functionalized ZnCQDs nanocomposites ECL probe	HA	Breast cancer	PBS buffer	1 cell	1–12 cells 1–18 cells	[8]
	$Ru(bpy)_3$-BO_3 labeled glycosyl-imprinted microshpheres	HA	CD44v6	Serum	0.08 ng L^{-1}	0.1–1000 ng L^{-1}	[35]
Fluorescence	FRET-based PFEP/FA-HA complex	HA	Breast cancer	Serum	3.5×10^{-8} g mL^{-1}	0–1×10^{-7} g mL^{-1}	[40]
	FRET-based of CD44/RHAMM	HA	Breast cancer	PBS buffer	–	–	[41]
	QD-conjugated antibody cytometry	HA	Breast CSCs MCF-7	Buffer	–	0.3–0.6% of 10^4 cells	[45]
	Fluorescence polarization (FP) technique by BIO probe	HA	Human cervical cancer (HeLa)	Homogeneous solution	~ 85 cells mL^{-1}	2.5×10^2 to 1×10^6 cells mL^{-1}	[46]
	NPs-based pH nanosensor	HA	HeLa cells	Buffer	–	–	[47]
	MRI and NIRF techniques for HACE-based nanoprobe detection	HA	U87-MG and SCC7	*In vivo* imaging	–	–	[48]
	FA and HA ligands conjugated with carbon nanodots and PEI (FA-PEI-HA-CNDs)	FA, HA	A549 lung cancer	PBS	–	–	[49]

Table 2
The diagnosis of CD44 based on colorimetric and SPR/SERS biosensing approaches.

Biosensing Method	Strategy	Sample	Recognition motif	Cell	LOD	Linear range	Ref.
Colorimetric	Sandwich ELISA using the *anti*-CD44-exonv3 and *anti*-CD44-exonv6 antibody pairs	Serum	Antibody	CD44v3	6.2 ng/mL	125 ng/mL	[53]
	HA@Fe_3O_4@SiO_2 microspheres (HA-functionalized nanozyme	Buffer	HA	HeLa and T98G glioma	2.0×10^6 cells/mL	–	[54]
	AuNPs immunolabels with plasmon coupling microscopy (PCM)	Buffer	HA	MCF7 and SKBR3 breast cancer	–	–	[63]
SPR/SERS	Antifouling SPR based on HA grafting to Au electrode	Complex media	HA	D44	0.6 ng/cm^2	0.6–16.1 ng/cm^2	[64]
	Au-PEG-HA NPs based SPR	Blood	HA	MDA-MB-231 or BT-474	0.01% of cell	–	[65]
	SERS NPs/nanotags consisting of Rh6G, MGITC, and Cy5	PBS	Antibody	Breast cancer	–	0.5×10^6 cells	[69]
	Dual-mode-based (DNA-AuNPs probes) Localized-SPR (LSPR) biosensor	PBS	Antibody	CD44/CD24	450 pM	–	[72]
	AuNRs-based spectral imaging systems (PARISS)	Fresh medium	–	CD24, CD44, and CD49f	–	–	[73]
	AuNR@Ag-based SERS biosensor	Blood	–	Breast cancer	1 cell/100 μl	$10–10^4$ cell	[9]
	Multifunctional SERS nanotags	PBS	–	Breast cancer	–	–	[74]

cancer cells. The assembled ZnCQDs probes/AuNPs were decorated on the magnetic beads (MBs) and further conjugated to HA (Fig. 2A). In this regard, ZnCQDs enhanced the ECL intensity. Moreover, the GO/AuNPs interface also improved the stability of the platform and ECL performance. Folic acid (FA)-functionalized GO/AuNPs were used to capture the cancer cells. HA-functionalized probes recognized the single cancer cell through CD44 on their cell surface. The linear range (LR) of this strategy was 1 to 12 single cells of MCF-7 and 1 to 18 of MDA-MB-231 cells. In addition, the ECL intensity indicated the high expression level of CD44 in the MDA-MB-231 cells [8]. The strong quenching capability, high aspect ratio for modifications, high spectral resolution and highly sharp emission bands make GO a considerable choice for biosensing platforms [29–31]. Moreover, in the manufacturing of GO-based biosensors, the time-resolved fluorophores are suitable because they reduce the background noises and interference of the intrinsic fluorescence of serum proteins [32,33]. GO/AuNPs hybrid materials with unique physico-chemical properties can act as quencher of fluorescence dye. Given its super-quenching feature, GO can be used to improve sensitivity and reduce background signals in fluorescent aptasensors [34]. The GO-serum proteins interactions alter the sensitivity of the sensing scaffold, which is a disadvantage for biosensing systems based on GO.

In 2021, a multi-probe ECL technique was developed for the CD44v6 detection by means of magnetic glycosyl-imprinted microspheres (MGIP) consisting of glycosyl-imprinted polymer//Au@Fe_3O_4/HA. The MGIPs were deposited on magnetron-controlled GCE (MGCE), which can selectively capture CD44v6 by the linking of the imprinted cavities to the HA (Fig. 2B). Tris (bipyridine) ruthenium (II) ($Ru(bpy)_3$-BO_3), as a luminophore was captured on the HA/CD44v6. The ECL response detected CD44v6 in serum samples with a LOD of 0.08 ng L^{-1} [35].

The luminescence-based CD44 biosensing performance confirm the ECL-based devices could be detected CD44 with high sensitivity at the range of nM. The cytotoxicity and weak photo-chemical stability are among shortcomings of ECL-based biosensors. Upconversion nanoparticles (UCNPs) as recent ECL emitters have exhibited remarkable benefits including low toxicity, light stability, high quantum yields, narrow emission peaks, and large anti-Stokes shift which make them suitable for a variety of area counting biotic imaging, labeling, and clinical treatment [36].

2.2. Fluorescence-based CD44 biosensors

The term of fluorescence refers to a kind of photoluminescence which is initiated by emit of the photon during the electronic transition as energy source [37]. Fluorescence-related approaches are among important optical systems and highlighted for a wide range of biosensors due to their enhanced sensitivity, reproducibility, less response time and non-destructiveness [38,39]. Incidentally, some researchers are interested using the fluorescence-based biosensing for the CD44 detection (Table 1).

A Förster resonance energy transfer (FRET)-based method was

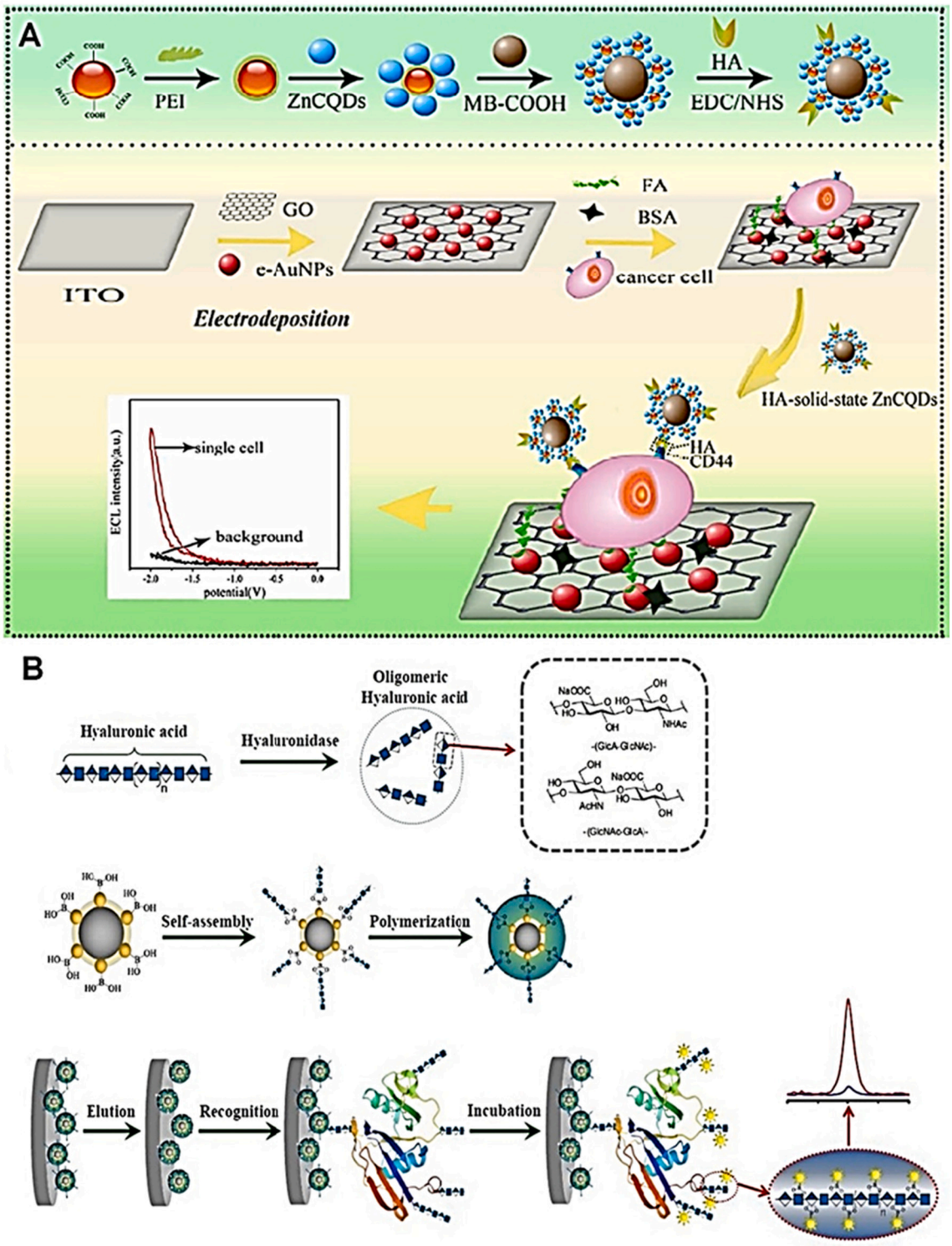

Fig. 2. A) The preparation process and the analysis mechanism of CD44-based cancer cells detection by HA-solid-state ZnCQDs nanocomposites ECL probe. B) A Ru $(bpy)_3$-BO_3 labeled glycosyl-imprinted polymer ECL sensor for CD44v6 determination in serum samples. Reprinted with permission from [8,35].

described for sensitive and naked-eye monitoring of CD44 and CD44-containing cancerous cell, by means of a cationic conjugated polymer (CCP)-PFEP probe and fluoresceinamine-HA (FA-HA). The formed PFEP/FA-HA complex generated a highly effective FRET from PFEP to FA-HA. Addition of CD44 resulted in binding of HA to CD44, thereby separating FA-HA away from PFEP and thus reducing the emission (Fig. 3A). In this method, a fluorescent blue color was visually observed by UV lamp from solutions containing a mixture of the sample and PFEP/FA-HA complex overcoming the need for a difficult and costly protein-labeling for CD44 detection. Above all, the combination of the high-amplified PFEP and the specific binding of HA-CD44 would render the system high sensitivity and specificity with an LOD of 3.5×10^{-8} g mL^{-1}, and can be used for valid quantitative detection of CD44. Moreover, the CD44-targeted uptake of PFEP/FA-HA NPs by MCF-7 cells suggested a dual-color tumor-targeted imaging probe for early diagnosis of cancer [40]. In another study, a FRET-based biosensing platform

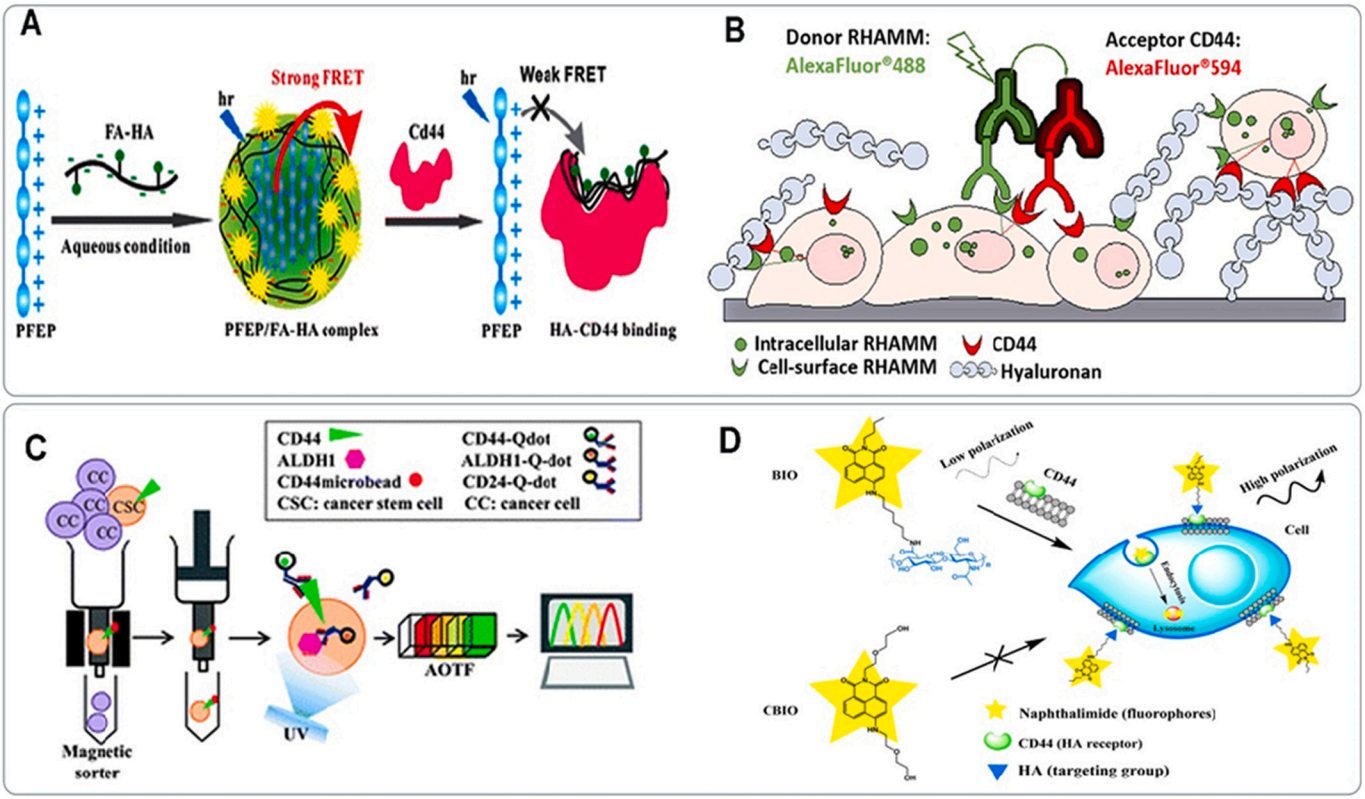

Fig. 3. A) Schematic design of the PFEP/FA-HA FRET-based strategy for CD44 detection; B) The scheme of the FRET-based assessment of CD44/RHAMM in breast cancer cells cultured on tissue culture polystyrene (TCPS) supplemented with dissolved and immobilized HA; C) The breast CSCs biomarkers detection based on QD-conjugated antibody using single cell imaging cytometry; D) The detection of CD44 based on fluorescence polarization (FP) technique by BIO probe. Reproduced with permission from [40,41,45,46].

combined with immunocytochemistry was reported in which HA was replaced with the association between RHAMM as donor and CD44 as acceptor. In this platform, CD44/RHAMM complexation was assayed in breast cancer cells seeded on tissue culture polystyrene (TCPS) supplemented with soluble and immobilized HA. In the presence of CD44 and RHAMM, the FRET signal was observed (Fig. 3B). CD44/RHAMM complexation was enhanced in all cell lines upon interaction with immobilized HA compared to its soluble form [41]. In the FERT-based assays, the optimization of the interference and the distance between the donor-acceptor molecules should be noted [42].

CSCs are a rare immortal subset of cancerous cells to be found within tumors and has self-renewal differentiation capacity similar with normal stem cells involving in the onset and relapse of cancers. Findings demonstrate that CSCs can possess good potential as a target in the detection, treatment and prevention of tumor invasion [1,10,11]. The CD44/CD24 ratio is the actual clinical significance in cancer, which is applied to categorize stem-like cancer cells. The CD24 is associated with adhesion and metastasis and appears at the surface of most B-cell lymphoma and neuroblastic tumors, while CD44 is required for cell-ligand interactions, adhesions of cell and is commonly expressed in different mammalian cell types [43]. The high expression of CD44 are observed in breast cancer-initiating CSCs and thus, CSCs-related CD44 can be suitable as a diagnostic biomarker for the breast cancer detection in early stage employed for therapeutic purposes. Cho et al. reported that polyvalent-directed peptide polymer (PDPP) that precisely identified CD44, could be used as a new method to detect breast CSCs [44]. In an interesting study, the breast CSCs were colorimetrically identified based on concurrent monitoring of QD-conjugated CD24, CD44, and aldehyde dehydrogenase 1 (ALDH1) by an acousto-optic tunable filter (AOTF)-based cellular imaging (Fig. 3C). The crucial defy for the synchronic revealing of several CSCs biomarkers is the overlaps between broad emission spectrum of the different fluorescent probes limiting the choice of accurate probes. In this study, each breast CSCs biomarker was differentiated based on specific fluorescence spectra resulted from antibodies of CD24, CD44, and ALDH1 labeled with Q-dot565, Q-dot525, and Q-dot625 (fluorescent dye), respectively [45].

Fluorescence polarization (FP) as a self-referencing fluorescence signal has substantial advances in fluorescence intensity-based sensing without depending on fluorophore concentration and environmental interferences. However, the common FP probes such as rhodamine, fluorescein, and cyanine dyes display a rather shorter excited-state lifetimes in comparison with naphthalimide and BODIPY dyes. Jia et al., for the first time, applied a naphthalimide, a relatively longer excited-state lifetimes, as a FP probe (BIO) for selective, direct, real-time, and quantitative detection of CD44-expressing human cervical cancer (HeLa) cells in homogeneous solution (Fig. 3D). The LOD was ~85 HeLa cells mL^{-1} with LR from 2.5×10^2 to 1×10^6 cells mL^{-1} within ~25 min. The relatively high photostability of naphthalimide can make the HA-modified BIO appropriate for identification of the CD44 expression live cell with confocal microscopy [46].

The NPs-based drug delivery systems that are conjugated to specific ligands provide a promising strategy for the therapeutics delivery to tumor cells. To determine the role of CD44 in the internalization of NPs to cells, a NPs-based pH nanosensor was synthesized that targeted CD44 on HeLa cells by using polyacrylamide NP matrix bearing HA ligand (Fig. 4A). The nanosensors were designed by NPs polymerization modified with pH sensitive and insensitive fluorophores and coated with HA. The pH distribution in cells was calculated for HA- and cationic-coated and neutral nanosensors. The imagining of nanosensor-containing cells indicated the CD44-mediated internalization of HA-coated nanosensors [47]. In another study, a nanosized HA-ceramide (HACE)-based probe was used for optical and magnetic resonance

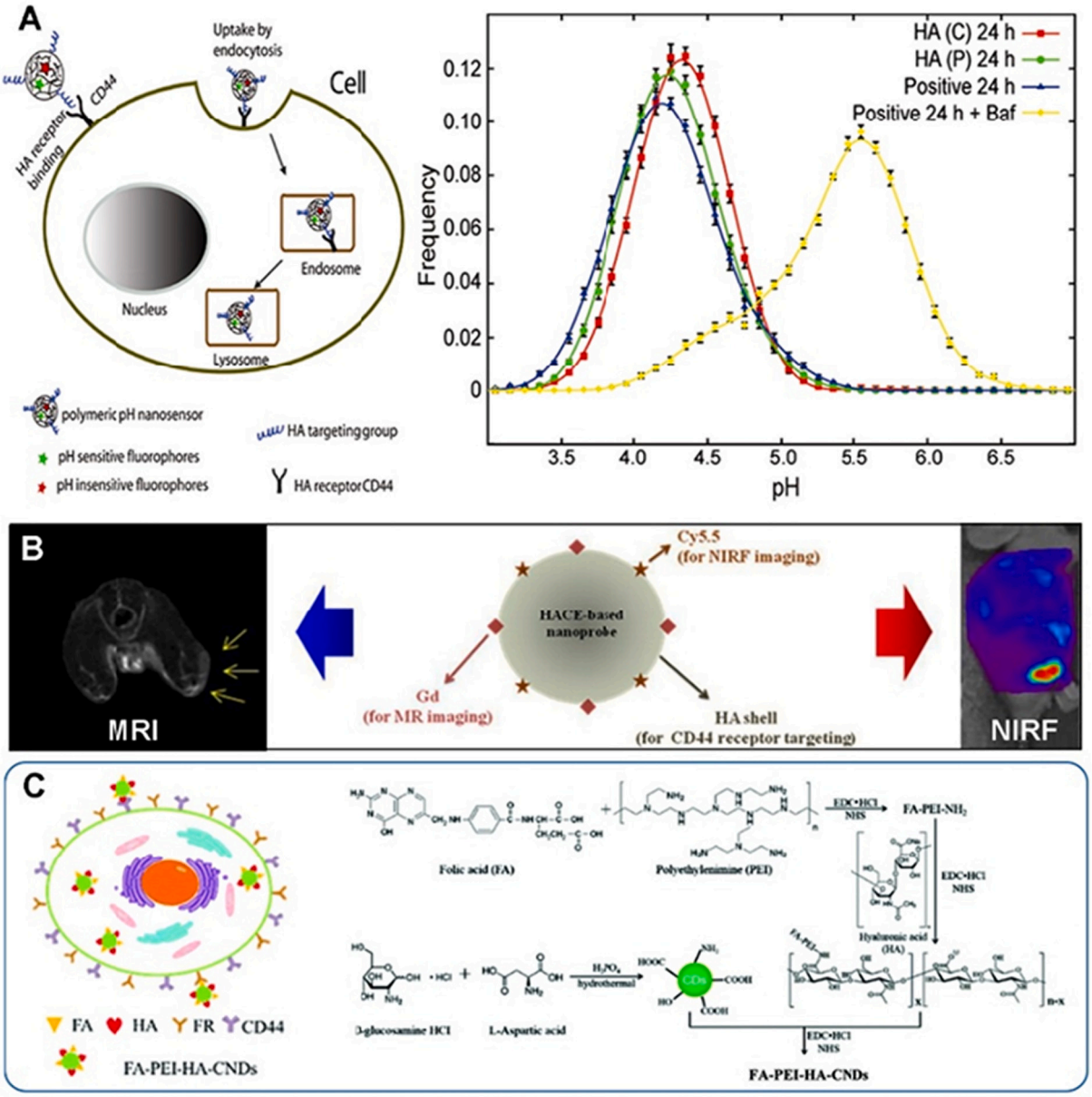

Fig. 4. A) Illustration of the nanosensor cellular internalization; B) The MRI and NIRF techniques based on HACE nanoprobe for the detection of CD44 expression SCC7 cells; C) The FA/CD44 based detection of cancer cell by with FA and HA ligands conjugated with carbon nanodots and PEI (FA-PEI-HA-CNDs). Reproduced from [47–49] with permission from the Elsevier.

imaging (MRI) of cancer. Herein, HACE nanoprobe was provided with its modification by pentetic acid (DTPA) as gadolinium (Gd) chelating agent and Cy5.5 as a near-infrared fluorescence (NIRF) imaging dye (Cy5.5-HACE-DTPA-Gd). The *in vitro* and *in vivo* outcome indicated an HA-CD44 interaction in SCC7 cells (CD44 positive) compared to U87-MG (CD44 negative) in tumor-bearing xenograft mice by MRI and NIRF imaging (Fig. 4B). Thus, this dual-mode imaging method can be used as a precise diagnostic system for CD44-positive cancer cells [48]. A dual FA/CD44 ligand-decorated nanocarrier was prepared by using the covalent conjugation of green-emitted fluorescent carbon nanodots (CNDs) with FA, polyethylenimine (PEI) and HA (FA-PEI-HA-CNDs) for the cancer cells imaging (Fig. 4C). The coupled FA-PEI-HA with CNDs showed the proper fluorescence intensity introducing it for the rapid and efficient diagnosis of real-time and noninvasive form of A549 as a lung cancer cells which are useful for cancer detection and drug delivery [49].

Although exciting progress has been made in the detection of CD44, using luminescence and fluorescence biosensors, the intrinsic fluorescence originated from serum proteins may interfere with the sensor function, hence fluorophores with time-resolved fluorescence characteristics should be utilized [50].

2.3. Colorimetric-based CD44 biosensors

Colorimetric-based biosensors have attracted numerous attentions for the detection of biomolecules owning to their output signal (color change) which can be easily visualized with naked eye [51,52]. Table 2 shows some examples of CD44 colorimetric biosensing.

A colorimetric sensing based on *anti*-CD44-exonv3 and *anti*-CD44-exonv6 antibody pairs was reported for the determining of serum CD44v3 with the LOD of 6.2 ng/mL and the LR of 125 ng/mL [53]. Another simple colorimetric procedure for the determination of HeLa and T98G glioma tumor cells was established based on a HA-functionalized nanozyme. The Fe_3O_4 NPs-immobilized mesoporous

silica microspheres (Fe_3O_4@SiO_2 microspheres) were conjugated to HA *via* carbodiimide activation (HA@Fe_3O_4@SiO_2 microspheres). This complex also acted as a peroxidase-mediated nanozyme, functioning *via* immobilized Fe_3O_4 NPs by converting the synthetic substance (3,3′,5,5′-tetramethylbenzidine, TMB) to a colored oxidized TMB as a basis of colorimetric assay. In the presence of CD44 expressing cells, the targeted complex was internalized into tumor cells and the peroxidase-like activity of nanozyme was declined which is related to the cell number. Thus, the proposed method determined the CD44-positive cancer cells by simply quantifying the visible absorbance of sample which can be an alternative for complex platforms [54].

In the presented CD44 commercial detection kits, ELISA test as a colorimetric assay is commonly used. However, limited researches have been done on colorimetric-based CD44 biosensors. Moreover, other biosensing methods showing similar performance with viable CD44 detection kits, are in the nascent stage. The limitation of antibody-based assays, for instance high sample volumes, cost of equipment and antibodies, timely assay can limit their application [55,56]. AuNPs have potential as proper candidate for the design of colorimetric-based biosensors for CD44 assays due to their higher sensitivity than organic dyes [52]. It should be mentioned that when AuNPs-based sensors are employed to identify targets in complex specimens such as serum, a phenomenon known as "corona shield effect" commonly occurs. This problem can be solved by including PEG molecules into the construction of biosensors [57]. Considering the incorporation of an isothermal and portable strategy in its framework, colorimetric biosensors can be used in the creation of profitable detection systems [58]. Simultaneous target identification and signal amplification plus visual target sensing using AuNPs, and thermo-stability has led to the straightforward operation of this sensor.

2.4. SPR/SERs-based CD44 biosensors

Surface plasmon resonance (SPR) as a bioaffinity optical biosensors analyzes the binding of targets to its receptors on the sensor surface in a label-free manner [59]. The sensing principle of the SPR-based sensors includes the reflective index change when the mass of targets bound on the surface of the biosensor is detected by SPR *via* resonance angle change of the reflected light [60,61]. NPs improve the sensitivity and signal enhancement of SPR sensors through enhancement of the reflected light index [59]. At present, various SPR-based biosensors are reaching a maturity level sufficient for the detection and determination of CD44 in clinical samples which are introduced in this section and summarized in Table 2. For the improvement of the SPR bioaffinity to targets, the sandwich-type SPR biosensors exhibiting excellent sensitivity and specificity, can be an ideal option which allows binding to different sites of the similar target *via* a pair of receptors [60,62].

A mix of AuNPs immunolabels with plasmon coupling microscopy (PCM) was employed to quantify the CD24/CD44 expression on breast cancer cells (MCF7 and SKBR3). The membrane distribution of CD24/CD44 was visualized with colors scales from green to orange [63]. Antifouling surfaces minimizing the adsorption of nonspecific protein are important for the development of the desired SPR biosensors. In a study, the covalent bond of a carboxylated HA to Au electrode provided an antifouling SPR platform with low protein adsorption of 0.6–16.1 ng/cm^2 among nonspecific proteins (Fig. 5). This research provided a promising SPR biosensor for the specific monitoring of CD44 biomarker and $CD44^+$ cancer cell in complex media due to the resistance of Au surface to nonspecific proteins adsorption [64].

Identification of rare cells of interest from a mixture of dissimilar cells shows the importance of the biomarker-based diagnosis of cancer cell. Rauta et al. reported a SPR platform to detect/isolate viable cells in human blood samples based on ligand-receptor chemistry using AuNPs coated with polyethylene glycol (PEG), conjugated with HA (Au-PEG-HA NPs) (Fig. 6A). In the presence of CD44, NPs were attached to cells generating a strong colorimetric change in the solution along with an additional shift of SPR peak from 521 nm to 559 nm. This AuNPs-based SPR nanosensor can support a point-of-care (POC) diagnostic devices [65].

Surface enhanced Raman spectroscopy (SERS) is a surface-sensitive technique in which inelastic light scattering from molecules in an electromagnetic field, are adsorbed on the nanosized metallic surfaces allowing for direct identification of low levels of analytes with an excellent sensitivity/specificity [66–68]. SERS technique has a remarkable multiplexing ability owing to the 'fingerprint' Raman spectrum from each molecule [67]. Dinish et al. applied SERS NPs/nanotags consisting of Rh6G, malachite green isothiocyanate (MGITC), and Cy5, as an ultrasensitive nanoprobe for the simultaneous detection of biomarkers of breast cancer including epidermal growth factor receptor (EGFR), CD44 and TGFβ receptor type II (TGFBRII), respectively. The intra-tumoral injection of nanotags-conjugated specific antibodies exhibited distinct multiplex Raman peaks (1120 cm^{-1} for TGFbRII, 1175 cm^{-1} for CD44 and 1650 cm^{-1} for EGFR biomarker) and revealed maximum SERS signal after only 6 h. In future, the proposed SERS nanotags can help the simultaneous detection of biomarkers and can be used as a theranostic probe for monitoring of tumor progression and therapy [69].

Lee research group identified the CD44 and CD24 biomarkers of breast CSCs, especially $CD44^+/CD24^-$ subpopulation by dual-mode-based localized-SPR (LSPR) biosensor. LSPR is produced from the

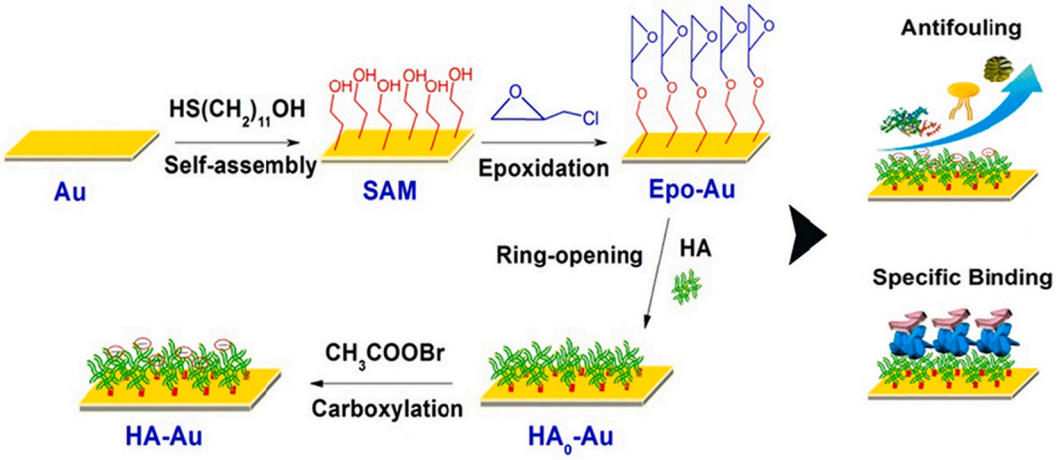

Fig. 5. Schematic Illustration of SPR consisting of HA grafted onto the Au surfaces. Reproduced with permission from [64].

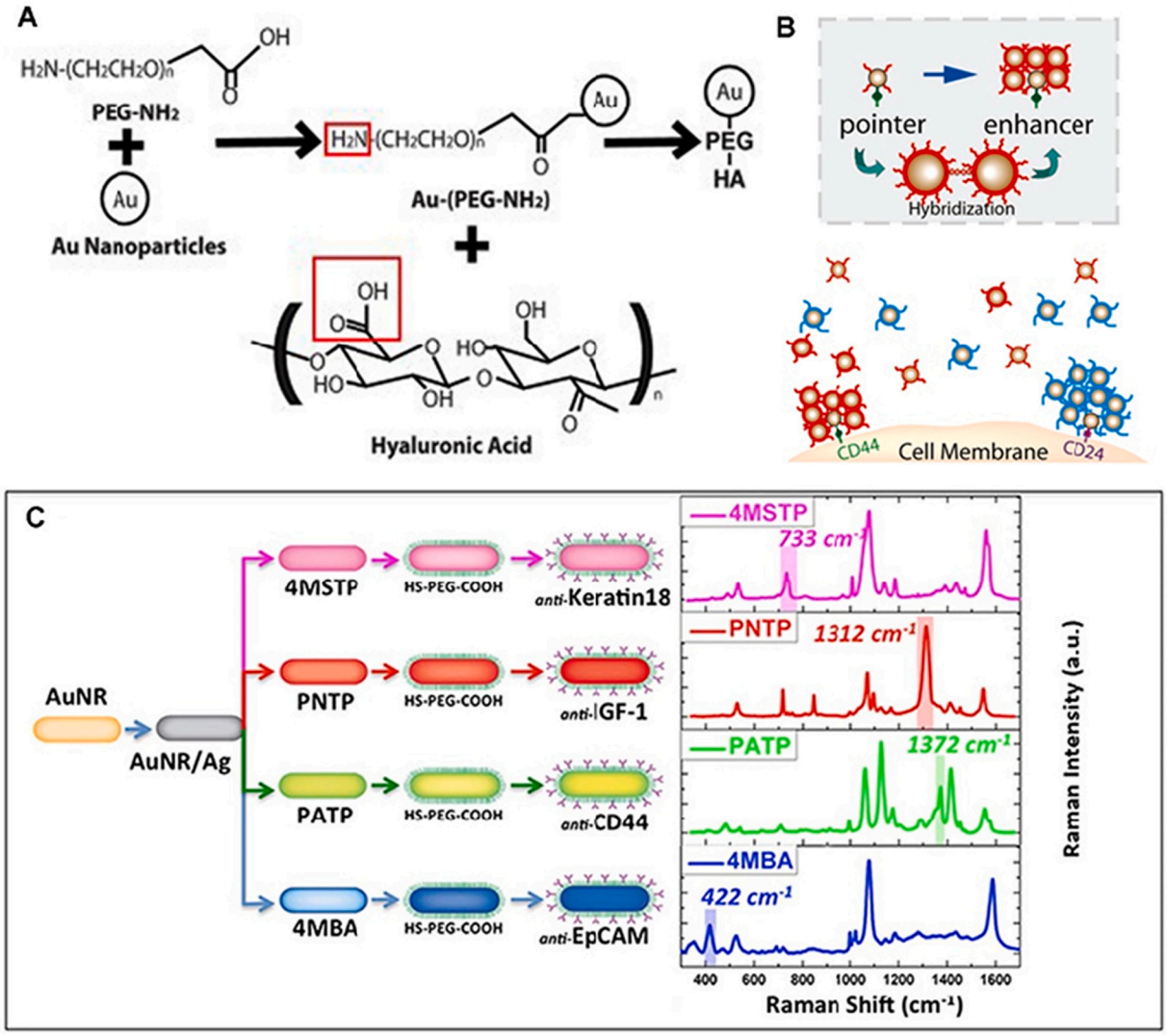

Fig. 6. A) AuNPs-based colorimetric and SPR biosensing methods for the detection and isolation of CD44 positive cancer cells; B) The CSCs biomarker detection strategy based on ssDNA/AuNPs probes consisting of receptor pointer particle and SERS signal enhancer particle; C) SERS technique for cancer biomarkers detection based on Ag-coated AuNRs modified with unique Raman tag and non-overlapping peak of each SERS signal. Reproduced with permission from [9,65,72].

interaction of light with surface electrons of conductive NPs. In comparison with SPR, the operation of LSPR platforms are simpler and more compact [70,71]. In this innovative study, a LSPR platform based on DNA-AuNPs probes was created to detect the CD24 and CD44 biomarkers. The DNA-AuNPs probes had two units including a) a pointer particle modified by anti-CD44 or anti-CD24 antibodies and single-strand DNA (ssDNA) and b) an enhancer particle consisting of Raman tags and complementary ssDNA (Fig. 6B). When pointer particles are attached to CD44/CD24, enhancer particles accumulated its surrounding *via* DNA hybridization, which provided a detectable signal with SPR and SERS. The designed nanosensors can be well-controlled enabling the sensitive multiplex detection of cancer cell membrane biomarkers [72]. Yu and colleagues provided a spectral imaging system (PARISS) for the detection of CD24, CD44, and CD49f biomarkers attached to gold nanorods (AuNRs). AuNRs appeared as a light spot in dark field images helping the biomarkers detection [73]. Another AuNRs-based SERS biosensor was used for the detection of keratin 18, epithelial cell adhesion molecule (EpCAM), CD44, and insulin-like growth factor 1 (IGF-1) receptor β, as breast cancer biomarkers in blood sample using silver (Ag)-coated form of AuNR (AuNR@Ag). For the identification of each biomarker, AuNR@Ag individually bound to a unique Raman tag and a specific antibody. In the CD44 approach, *p*-aminobenzoic acid (PATP) was used as Raman reporter molecule, which was coated with PEG and generated a SERS signal at 1372 cm^{-1} (Fig. 6C). This SERS-based CTC (circulating tumor cell) detection can be considered as POC diagnostic system for on-site, simple, high specific and rapid detection of cancer [9].

Another multifunctional SERS nanotag was used to recognize co-expressed breast cancer biomarkers including CD44, ErbB2, and EpCAM. In this procedure, three PEGylated Au—Ag hollow nanospheres were labeled with distinct tags such as Rhodamine B isothiocyanate (RBITC), MGITC and 3,3-diethylthiadicarbocyanine iodide (DTDC) to increase the surface electromagnetic fields of Raman reporter molecules. The SERS mapping images revealed a red color with a peak at 1646 cm^{-1} in Raman signal spectrum for CD44. The assayed SERS nanotags can provide a high-resolution multiplexed live cell image and fast and accurate detection of breast cancer cells [74].

SPR-based approaches have been accompanied with some shortcomings such as their affinity to non-target molecules with similar structure of target, insufficient resonance strength, and the background refractive index, limiting their use for the detection of CD44 in multiplex samples [71]. Therefore, upgrading of the sensitivity and specific binding of the SPR, SERS, and LSPR biosensors is an urgent requirement for the precise detection of CD44 from coexisting biomarkers in samples.

3. Electrochemical-based CD44 biosensors

An electrochemical biosensor is an amalgam of the bioreceptor and a transducer which measures and processes the signal (current) produced from a biochemical reaction in close proximity to the electrode surface [75]. NPs increase the output signals and the sensitivity of biosensors by adjusting the electrodes surface and speeding up the electron transfer through the electrode [76]. Amperometric, impedimetric, potentiometric, and conductometric are known as kind of electrochemical biosensors [75,77]. These biosensors are remarkably used for the detection of cancer biomarkers because of their fast, robustness, easy miniaturization, excellent sensitivity and selectivity properties [78,79]. This section highlights a series of sensitive and specific electrochemical platforms, which have been developed for the detection of CD44, alone or simultaneously (Table 3).

Eissa et al. defined a label-free electrochemical immunosensor for liver CSCs based on CD90, CD44, OV-6 and CD133/2 biomarkers using their specific antibodies. To fabricate the platform, the biomarker-specific antibodies were covalently immobilized on Au electrodes *via* isothiocyanate linker. The CSCs binding on the sensor surface prevents the transfer of electron between $[Fe(CN)_6]^{3-/4-}$ redox probe and the Au electrode, thus increasing the detectable charge transfer resistance (R_{ct}) *via* electrochemical impedance spectroscopy (EIS). The developed immunosensor can specifically monitor CSCs with a wide LR from 1×10^1 to 1×10^6 cells mL^{-1} with LOD of 1 cell mL^{-1}. This platform showed a simple, sensitive, and precise manner for liver CSCs detection, offering the opportunity for early diagnosis or screening patients with metastatic liver cancer [80,81]. An asymmetric multiplex ligation-dependent probe amplification (MLPA)-based electrochemical sensor was fabricated to detect CD24, CD44 and some other breast cancer biomarkers. In the MLPA reaction, one pair of primer can amplify the multiple targets. In this study, a standard printed circuit board (PCB) technique was used for the fabrication of Au-based microarray electrodes followed by immobilization of the synthetic MLPA probe as a unique barcode sequence, on each electrode, which is hybridized with ssMLPA amplicon. The formed DNA duplexes were hybridized with a DNA probe-conjugated HRP followed by the addition of a TMB substrate, which was sensed using electrochemical pulse amperometry. The PCB fabricated microarray-based electrochemical platform showed the low-cost, specific and simultaneous detection of biomarkers as well as enhanced performance of sensor, which was equal to planar photolithographically-fabricated Au electrodes. The LODs calculated for this sensor were 258 pM and 161 pM for CD24 and CD44, respectively [43].

For the first time, a photoelectrochemical (PEC) platform was fabricated for the detection of CD44 in serum based on the antifouling effect of immobilized HA/PEG on the polydopamine (PDA)-coated TiO_2 substrate (Fig. 7A). The soluble CD44 was recognized with immobilized HA which decreased the TiO_2 PEC signal with a wide LR from 5 to 5×10^5 pg mL^{-1} and a LOD of 0.44 pg mL^{-1} of CD44. The development of a biosensor capable of detecting soluble CD44 can pave the way for the recognition and handling of malignant cancers [82]. In a report, Zhao et al. described multiple signal amplification strategy based on the self-assembled supramolecular diphenylalanine (FF)-AuNPs nanocomposites for the electrochemical detection of CD44 on breast CSCs. In this platform, an Au electrode was functionalized by trypsin-digestive CD44 binding peptide (CD44BP). When CD44 was added to the system, CD44BP was protected from enzymatic degradation. The bound CD44 was replaced with cucurbit[8]uril (CB [8]) followed by conjugation of FF-AuNPs (Fig. 7B). After Ag enhancement, EIS signal was obtained with a LOD of 2.17 pg mL^{-1} for CD44 and 8 cells mL^{-1} of $CD44^+$ breast CSCs [83]. The amount of serum level of CD44 is linearly related with some of cancer-specific clinicopathological factors.

A sandwich-type electrochemical cytosensor is designed to quantify the CD44-positive HeLa cells. Herein, the conjugated HA into multi-walled carbon nanotubes (MWCNTs)-modified indium tin oxide (ITO) electrode along with HA-modified fluorescent probe (named as BIO) were used to form an appropriate sandwich sensing platform (Fig. 8A). The 3D-MWCNT speeds up the electron transfer ratio and surface chemical reactivity. The signal amplification was measured by chronocoulometry (CC) differential pulse voltammetry (DPV). The attachment of CD44-positive HeLa cells to the HA@MWCNT/ITO decreased the CC and DPV response, whereas adding the BIO-labeled HA exhibited a maximum response with a LOD of 70 cell mL^{-1} [84]. A label-free electrochemical sensor for CD44 was introduced based on assembled MWCNTs composites on the electrode surface to progress the conductivity. HA was coupled to MWCNTs by using poly(diallyldimethylammonium chloride) (PDDA) (Fig. 8B). The CD44-positive cells were directly detected in human serum with a LR of 0.01–100

Table 3
Electrochemical biosensors for the detection of CD44.

Approach	Recognition unit	Cell	Sample	LOD	LR	Ref.
Label-free immunosensors based on antibody-immobilized on Au electrodes	Antibody	Liver CSCs	Buffer	1 cell mL^{-1}	1×10^1 to 1×10^6 cells mL^{-1}	[80,81]
MLPA-based sensor by Au-based microarray electrodes	MLPA probes	Breast cancer	Buffer	258 pM CD24 161 pM CD44	–	[43]
Diphenylalanine (FF)-AuNPs nanocomposites	CD44BP	Breast cancer	Buffer	2.17 pg mL^{-1} CD44 8 cells mL^{-1}	0.01–100 ng mL^{-1}	[83]
PEC biosensor based on Co-immobilized HA and PEG	HA	–	Serum	0.44 pg mL^{-1} CD44	0.005 to 500 ng mL^{-1}	[82]
HA@MWCNT/ITO	HA	HeLa cells	Buffer	70 cells mL^{-1}	2.1×10^2 to 2.1×10^7 cells mL^{-1}	[84]
ITO-MWCNTs-PDDA-HA sensor	HA	–	Serum	5.94 pg mL^{-1}	0.01–100 ng mL^{-1}	[85].
Magnetic particles functionalized with antibodies	Antibody	Breast cancer	Serum	10^5 exosomes μL^{-1}	–	[86]
LbL assembled Fe_3O_4@SiO_2@HA	HA	CD44	Serum	~0.6 ng mL^{-1}	1 ng mL^{-1} to 10 μg mL^{-1}	[87]
Label-free impedimetric based on HA and CHI LbL films	HA	Prostatic tumor cells	PBS	50 cells μL^{-1}	50 to 600 cells μL^{-1}	[88]
HA/L-Cys AZIS QDs/FePc-based PEC platform	HA	A549 cells	Buffer/ Serum	15 cells mL^{-1}	2×10^2 to 4.5×10^6 cells mL^{-1}	[89]
HA-TiO_2/Ti_3C2Tx/$BiVO_4$ heterojunction based PEC biosensor	HA	CD44	Buffer	1.4×10^{-2} pg mL^{-1}	2.2×10^{-4} ng mL^{-1} to 3.2 ng mL^{-1}	[90]
MNFs-bounded DBCO-AgNPs	CD44BP	Breast CSCs	Buffer	6 cells mL^{-1}	10 to 5×10^5 cells mL^{-1}	[91]
Bifunctional DBCO/QDs DNA probes-based biosensing	Antibody	Breast CSCs	Serum	0.0792 ng mL^{-1}	0.1–1000 ng mL^{-1}	[92]
HA-BSA-AuNPs nanocomposites label-free EIS sensor	HA	MDA-MB-231	Buffer	128 cells mL^{-1}	2×10^2 to 3×10^5 cells mL^{-1}	[93]

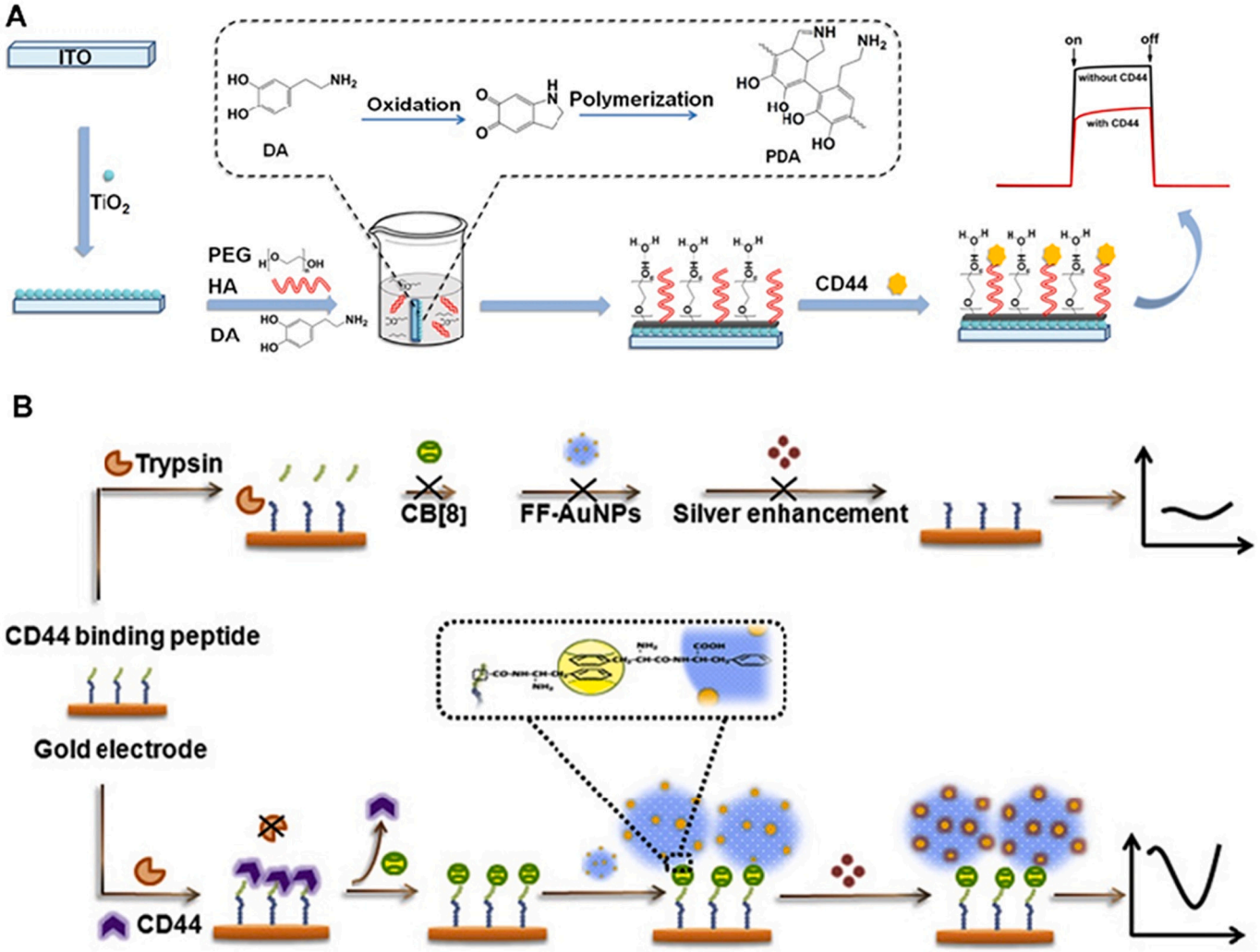

Fig. 7. A) A PEC-based biosensor for the determination of soluble CD44 using a co-immobilized HA as a detector unit and PEG as antifouling unit; B) An EIS method for CD44 detection based on FF-AuNPs nanocomposites and Ag enhancer. Reproduced with permission from [82,83].

ng mL^{-1} and a LOD of 5.94 × 10^3 ng mL^{-1} without requiring any labeling for signal amplification. The sensor showed reproducibility, high selectivity, and long-time stability [85].

An amperometric immunomagnetic sensing platform was developed to identify the breast cancer-derived exosomes by magnetic NPs modified with antibodies for exosome tetraspanins CD9, CD63 and CD81 and cancerous biomarkers CD24, CD44, CD340, CD54, and CD326. Exosomes are nano-sized vesicles, may serve as possible analytical approach for the detection of biomarkers related to various illnesses as well as cancers. In the serum of breast cancer cases, 10^5 exosomes μL^{-1} was detected *via* this procedure [86]. In other work, the layer-by-layer (LbL) assembled HA-functionalized magnetic particles (Fe_3O_4@SiO_2@HA) was used for the isolation and detection of CD44 in serum by mass spectrometry and electrochemical biosensing. The electrochemical sensing by means of HA-modified electrodes verified the HA-CD44 binding in buffer and serum samples with a LOD of ~0.6 ng mL^{-1} and a LR from 1 ng mL^{-1} to 10 μg mL^{-1} [87]. A impedimetric label-free sensing platform, as a POC method, was employed to detect prostatic tumor cells based on interdigitated electrodes modified with HA and chitosan (CHI) LbL films (Fig. 9A). Despite the low selectivity of the multilayer films, EIS assay showed that this platform could detect 50 to 600 prostate tumor cells μL^{-1} due to the specific interaction of HA on the outer layer of HA/CHI/HA films with $CD44^+$ cells, which was confirmed by the information visualization methods. Therefore, the processing of the CD44-HA interactions data by computational methods is useful for the analysis of LbL chip data and POC diagnosis of cancer [88].

In another research, L-cysteine-modified Ag–$ZnIn_2S_4$ QD (L-Cys AZIS QDs)-based PEC analytical platform was prepared to quantify CD44-positive cancer cell. To develop the PEC performance, iron phthalocyanine (FePc) was mixed with L-Cys AZIS QDs to form a L-Cys AZIS QDs/FePc amalgam with an efficient photoelectric conversion. The PEC responses were obtained under the irradiation of near-infrared range (NIR) light. Cancer cells are immobilized onto HA/L-Cys AZIS QDs/FePc hybrid *via* HA-CD44 linkage, thus decreasing the photocurrent intensity (low PEC signal) (Fig. 9B). The PEC platform was capable of determining of 15 A549 cells mL^{-1}. This PEC method was also able to detect other cancer cells expressing CD44 [89]. Interfacial charge-carrier recombination can restrict the efficiency of PEC biosensors in wearable clinical electronics. In a study, Soomro et al. proposed an approach based on photoactivity of $BiVO_4$, and conductive 2D-$Ti_3C_2T_x$ (titanium carbide/MXene) nanosheets for PEC biosensing of CD44. In this platform, a PEC heterojunction (TiO_2/MX-$BiVO_4$) was made between *in-situ* formed TiO_2-$Ti_3C_2T_x$ and lysine-functionalized $BiVO_4$ adsorbed on MXene nanosheets with minimal interfacial recombination and then functionalized with HA (HA-TiO_2/MX-$BiVO_4$) (Fig. 9C). The robust interaction of lysine-functionalized $BiVO_4$ and HA exhibited the antifouling features for mimic proteins *e.g.* PSA and NSE. The CD44 binding to platform inhibited the signal of ascorbic acid as a redox mediator. The biosensor

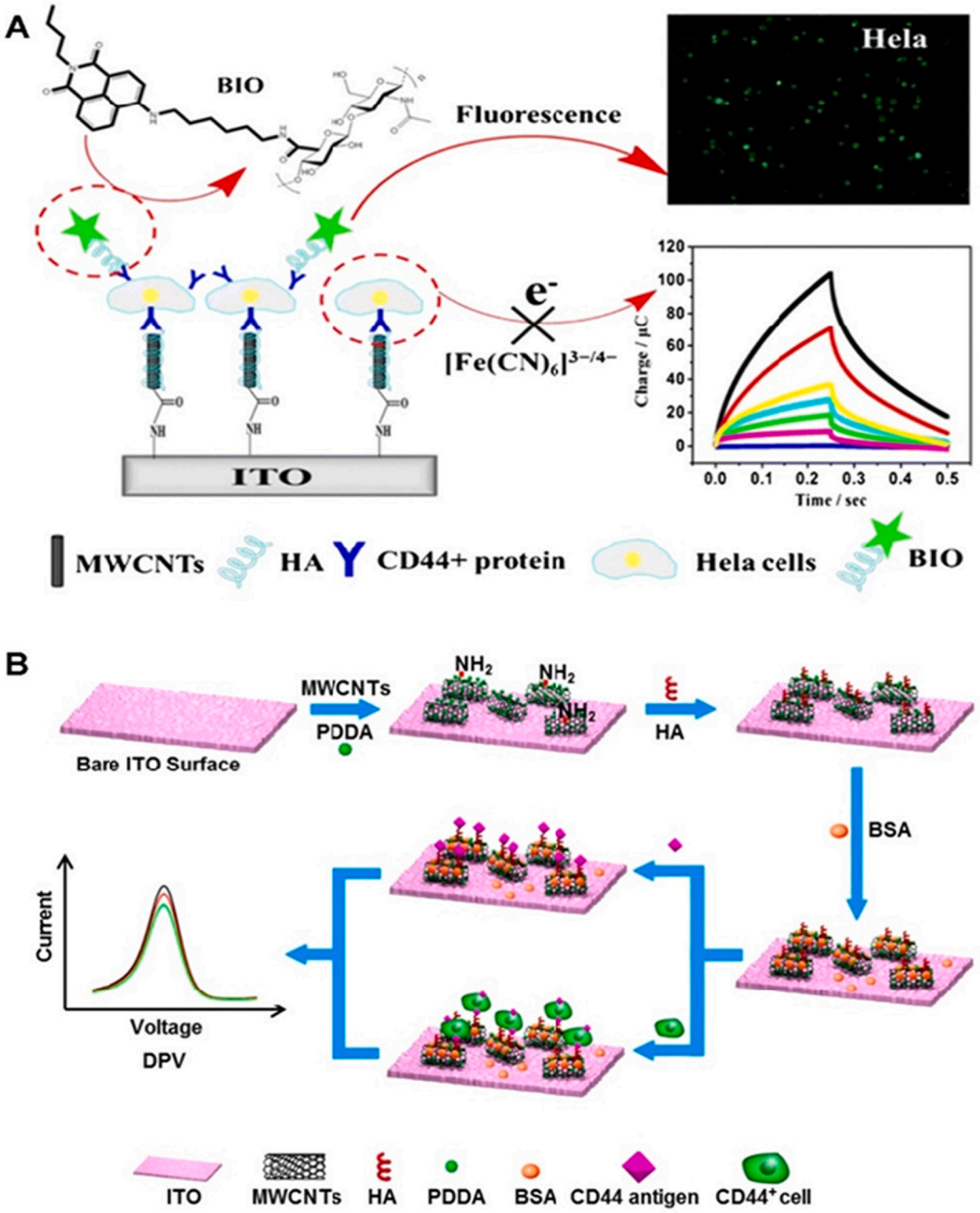

Fig. 8. A) The HA-MWCNT-based biosensing process for fluorometric and chronocoulometric assessment of $CD44^+$ Hela cells; B) A label-free sensing process for recognition of CD44+ cells by ITO-MWCNTs-PDDA-HA sensor. Reproduced with permission from [84,85].

recognized CD44 with LR in the range of ng mL^{-1} and a LOD of 1.4×10^{-2} pg mL^{-1}. The quantification of CD44 in real samples (blood/serum) can justify this PEC biosensor as ideal candidate for clinical purposes [90].

An electrochemical biosensor was designed to identify CD44-expressed breast CSCs in complex sample using the multifunctional nanofibers (MNFs) consisting of Aβ peptide and CD44BP (Fig. 10A). MNFs are involved in specific targeting of CD44, recruiting dibenzocyclooctyne (DBCO)-AgNPs as source of electrochemical response, and exhibiting the reaction sites to enhance the signals. The captured breast CSCs by AS1411 aptamer were detected by binding of CD44 to CD44BP unit of MNFs. Afterwards, the azide groups of MNFs contributed to the ligation of AgNPs as the signal labeling. Regarding the MNF-bounded DBCO-AgNPs signal, the platform selectivity detected minimum 6 cells mL^{-1} [91]. Another DBCO-based study followed a similar method, was designed based on bifunctional DNA probes for the recognition of CD44. In this project, an immune-complex was formed by hybridization of capture probes (DNA-CD44 antibody) after binding of probes with CD44 (Fig. 10B). The subsequent cyclic strand displacement reactions created the dual-labeled signaling probes with DBCO and CdTe-QD. These signaling probes play a role as bifunctional probes, not only specifically augmented on azide-coated MBs (azide@MBs) but also generated the electrochemical amplification of QDs. This approach provided a specific platform for the detection of serum-containing CD44 and CD44-positive breast cancer cells as well as for the monitoring of CD44 expression. In this assay, the LR of 0.1 to 10^{-3} ng mL^{-1} and LOD of 0.0792 ng mL^{-1} were obtained providing a robust instrument for the CD44 detection and offered a promising prospective for breast CSCs assessment in the future [92].

In 2021, a new label-free EIS sensor was constructed based on

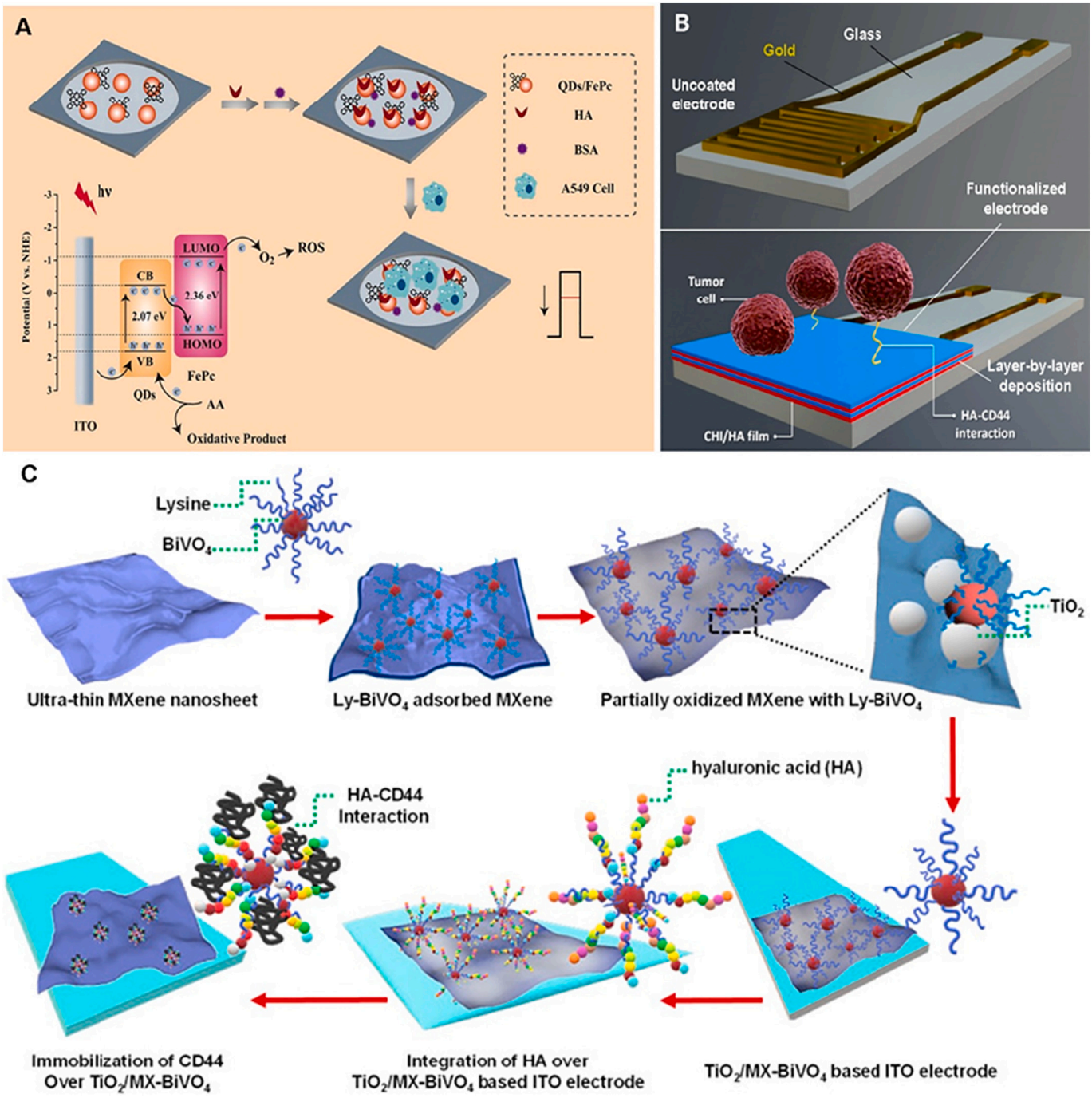

Fig. 9. A) The comparison of CHI/HA functionalized multilayer chip with uncoated electrode as well as the curves of CHI/HA electrodes after interaction of HA and CD44-positve tumor cell in various concentrations; B) A L-Cys AZIS QDs/FePc-based PEC cytosensor for CD44 detection; C) A TiO_2/MX-$BiVO_4$ (TiO_2/$Ti_3C_2T_x$/$BiVO_4$ heterojunction)-based PEC biosensor for CD44 detection. Reproduced with permission from [88–90].

conjugation of HA with bovine serum albumin (BSA)-modified AuNPs nanocomposites (HA-BSA-AuNPs) for the analysis of CD44 expression and cancer cell quantification. The $CD44^+$ cancer cells were deposited on the HA-BSA-AuNPs-functionalized GCE electrode by HA, enhancing the electron-transfer resistance (R_{et}). On the basis of quantified R_{et} by the EIS, the cancer cell number and CD44 expression level were estimated. Under optimum conditions, the EIS response was observed from 200 to 3.0×10^5 cells mL^{-1} with a LOD of 128 MDA-MB-231 cells mL^{-1}. Besides, the high expression rate of CD44 was observed in the MDA-MB-231 cells in comparison with L02 and HCT116 cells. This showed that the MDA-MB-231 cells had a greater metastatic potential as CD44 plays a critical role in metastasis process [93].

As claimed in previous studies, the LOD in the range of ng mL^{-1} obtained by electrochemical CD44 nanosensors indicates similar results compared to the commercial CD44 kits, which employ ELISA method. It should be noticed that the detection of low levels of CD44 in laboratory can guaranty its detection in real samples thus highlights the prospects of cancer detection in the early stages when CD44 is present in trace amounts.

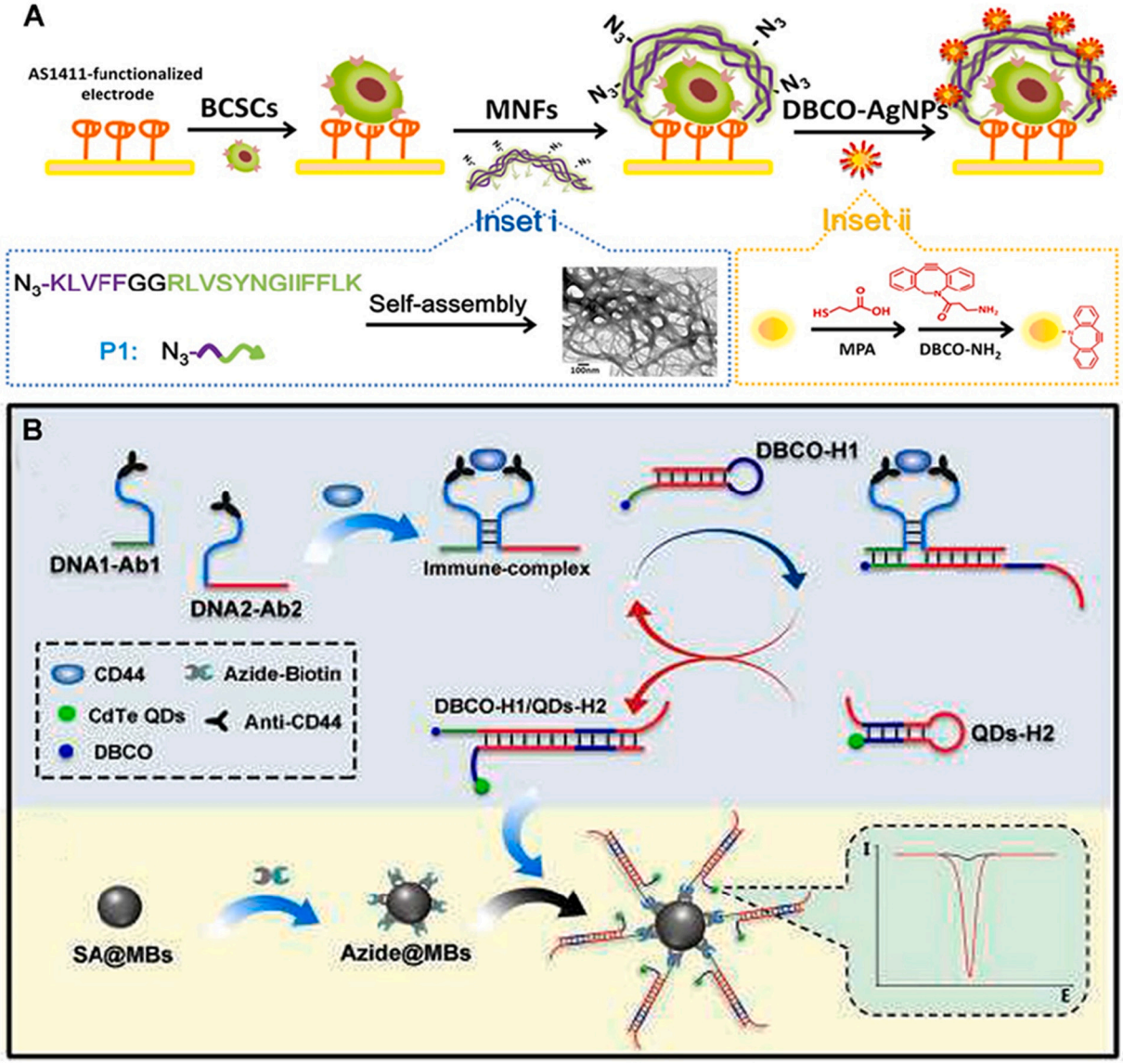

Fig. 10. A) The multifunctional nanofiber-based electrochemical detection of breast CSCs; B) Bifunctional DBCO/QDs DNA probes-based biosensing for identification of breast CSCs biomarker CD44. Reprinted with permission from [91,92].

4. Piezoelectric-based CD44 biosensors

Piezoelectric biosensors, for example, surface acoustic wave (SAW) sensors and quartz crystal microbalance (QCM) sensors as a mass-based devices are associated with the assessment of the mass variation on the surface of sensor, which leads to a shift in the resonance frequency (*f*) on a quartz. Structurally, in QCM, a quartz electrode is packed in the middle of metal (Al, Au, Ti, *etc.*) layers for electrical contact [94]. By attachment of analyte or any other mass on the surface of electrodes, an alternating electrical field is applied across the crystal resulting in change of oscillation frequency of the QCM device which can be detected by an accurate analyzer system [95]. The QCM-based bioassays have been commonly applied for various target detections including cancer and tumor marker detections [96]. The QCM sensor is best suited for biomarker detections (*e.g.* CD44) owing to portability, high sensitivity, short response time, ease of operation, low-cost, and real-time and label-free detection capabilities [97,98].

A QCM sensor was reported based on synthesized HA-modified magnetic NPs (HA-MNPs) for screening and detection of leukemia cells (CCRF-CEM). The cells were extracted from samples of human plasma based on particular binding of HA-CD44 with a LOD of 8×10^3 cells mL^{-1} [99]. Given the cellular communication upon mechanical stimuli, the single molecule devices were used to assay the mechanical forces arising from GAGs/protein bonds. Bano et al. developed QCM-based sensor, by combining of immobilized HA as a GAGs polymer on surfaces and CD44 at organized nanoscale system with single molecule force spectroscopy (SMFS) to study the interaction of HA/CD44, in vascular endothelium. Single HA-CD44 bond with low binding affinity showed high strength to rupture force in contrary to multiple bonds with low tensile resistance. It is also demonstrated that the strong non-covalent bonds, which are useful for HA immobilization, are considered as molecular anchors in SMFS [100].

Yang et al. defined a QCM-based sensing device for the investigation of metastatic potential of MDA-MB-231 (M-231) and MCF-7, as breast cancer lines by using HA, polydopamine and PEI composite film (HA/PEI/PDA), capturing CD44-positive cancer cells *via* HA-CD44 binding (Fig. 11A). The LOD for MDA-MB-231 and MCF-7 cells was obtained to be 300 and 10^3 cells mL^{-1}, respectively. The CD44 expression level on MB-231 cells was as twice as that of MCF-7 cells, representing its higher metastatic potential. Moreover, the metastatic potential of cells was

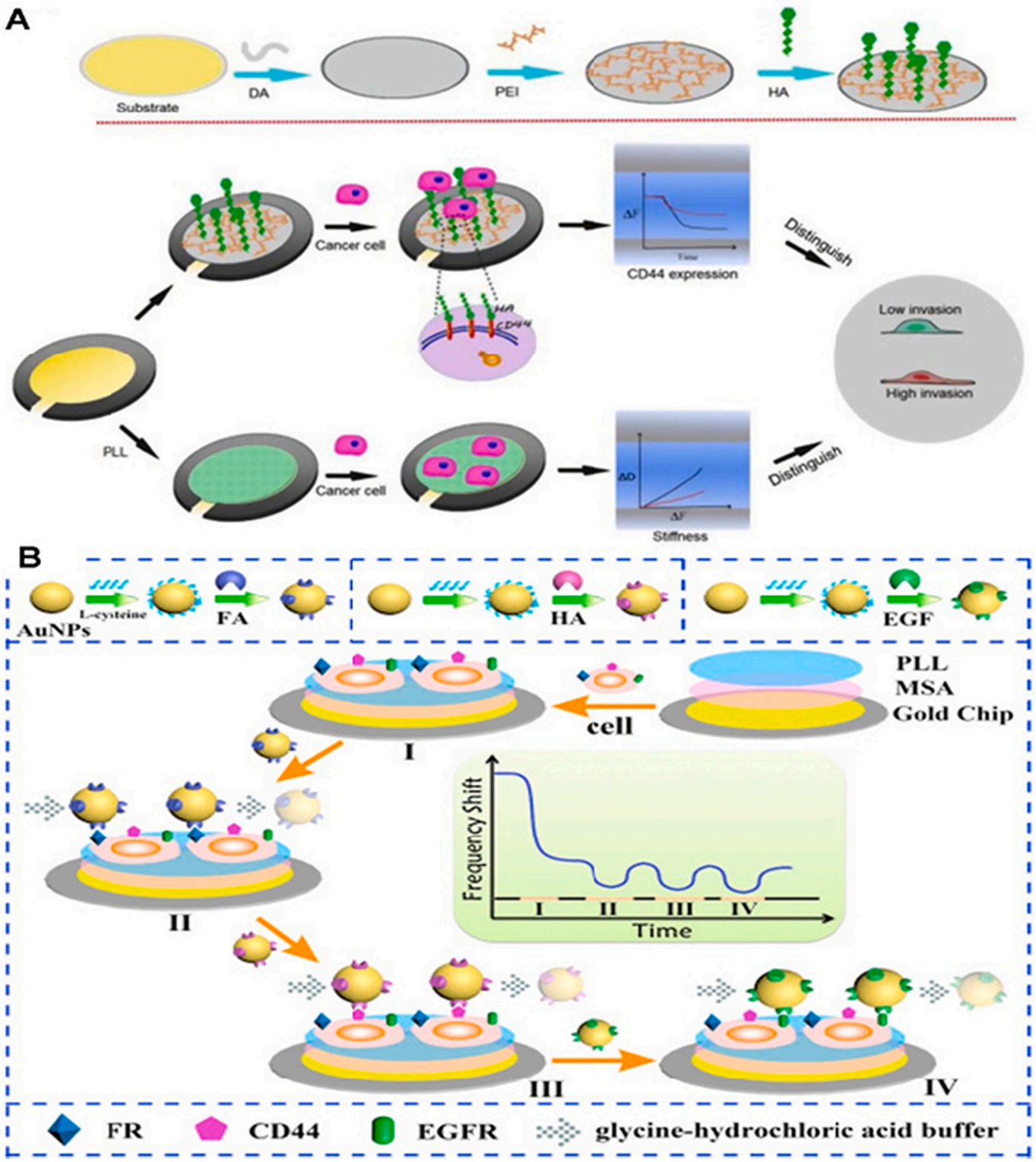

Fig. 11. A) The HA/PEI/PDA film-based QCM biosensor for assessing metastatic breast cancer cells; B) The simultaneous detection of FR, CD44 and EGFR by multianalyte QCM cytosensor using a signal recovery strategy. Reproduced with permission from [96,101].

assayed based on the rigidity of cancer cells by poly-L-lysine adjusted QCM sensor. The data revealed the high stiffness of MCF-7 in comparison with M-231 cells, indicating higher metastasis potency of M-231 cells [96]. A signal recovery-based QCM cytosensor was developed for the monitoring of multiple biomarkers including EGFR, FA receptors (FR), and CD44. In this study, the ligand-functionalized mass nanoprobes were obtained with conjugation of ligands (EGF, FA, and HA) with AuNPs (Fig. 11B). The elution of mass of nanoprobes linked to the surface of cell with glycine-HCl buffer, resulted in a fast recovery of resonance frequency. A LR of 3×10^4 to 10^6 cells and a LOD of 5×10^3 MDA-MB-231 cells were obtained by this method. Additionally, the sensor displayed three sensitive and recoverable frequency shifts, indicating the expression levels of EGFR, FR, and CD44 on cell membrane, demonstrating the mean of molecules of EGFR, FR, and CD44 per MDA-

MB-231 cell were 1.4×10^5, 0.5×10^6, and 0.2×10^6, respectively. Compared with monolithic multichannel QCM, the single microbalance-based cytosensor for multi-analyte analysis, acoustic interference can be excluded and thus introducing a modern tool for early cancer detection [101].

Amorim et al. reported an advanced LbL film by using poly-L-lysine (PLL) as well as different size and/or crosslinked HA for investigating the specific HA-related interactions. In this study, the assembled HA and its interaction with CD44 was characterized by QCM with dissipation (QCM-D), atomic force microscopy (AFM) and SPR. The existence of CD44 led to the cleavage of the non-crosslinked multilayers, while cross-linked films remained stable [102]. Table 4 presents QCM-based CD44 detection strategies.

5. Miscellaneous biosensing methods for CD44 detection

An AFM-based biosensor was designed based on HA-functionalized PEG-based hydrogel particles as soft colloidal probes (SCPs) for AFM to study the interaction between HA and CD44 (Fig. 12A). The selective binding of SCPs to CD44-positive cells was confirmed through AFM adhesion measurements [103]. Another SCP-AFM sensor was used to assay the effect of molecular weight (MW) of HA on the CD44-HA interaction (Fig. 12B). In this system, the 3D collagen (Coll I) matrices were modified with either low or high molecular weight HA (LMW-HA and HMW-HA) and then were exposed to CD44-positive and CD44-negative BRO melanoma cell lines. The cell adhesion measurements revealed the specific interaction of LMW-HA with $CD44^+$ cells [104].

6. Aptasensor-based CD44 detection

Aptamers are artificial single-stranded oligonucleotides selected from repeated cycles of an *in vitro* random sequences isolation called SELEX (Systematic Evolution of Ligands by Exponential Enrichment) suggesting as interesting alternatives to antibodies [105,106]. Aptamers offer special features for analytical aims *e.g.* cheap and fast production, vast specificity and sensitivity, target-based flexibility as well as stability in regards to unfolding, denaturation, and non-physiological situations [105,107]. In general, a conformational change in aptamers structure without need for extra labeling was observed when interacting with their targets [108]. Aptamers have recently successfully applied for the diagnosis of various biomarkers of cancer [109,110]. The isoforms of CD44, CD44s and CD44v, demonstrated different structures in cancer and normal cells (Fig. 1) [6]. CD44s consists of exon 1–5 (or S1-S5) and 16–20 (S6-S10), while CD44v carries the exon v1–10 (Fig. 1) [12,111]. This phenomenon may be important in the design of CD44 aptamers (Apt_{CD44}) and related aptasensors to differentiate tumor from normal cells. On this note, some anti-CD44 aptamers have been isolated based on different isoforms structure of CD44 (Table 5).

Ababneh et al. introduced an amended RNA aptamer, known as Apt1, against human CD44s isoform. In this study, a RNA aptamer was isolated by human recombinant full-length CD44 protein and 2¢-F-pyrimidine modified RNA library. The binding specificity of the selected RNA aptamer (2'-F-pyrimidine-containing Apt1) towards CD44-expressed cell lines including MCF7, MDA-MB-231, and T47D was confirmed by fluorescent microscopy and flow cytometry. It was also demonstrated that certain aptamers can be applied to target CD44-positive CSCs [112]. Two DNA aptamers developed against CD44v10 named as Apt#4 and Apt#7 were able to prevent the breast cancer cell migration. Further assays confirmed that these aptamers inhibited the interaction between the exon with EphA2. EphA2 involved in promoting tumor invasion and metastasis [113].

Breast CSCs are considered as a challenge in anticancer therapies due to their role in drug resistant of mammary tumor. The cell-SELEX approach was carried out to isolate ssDNA oligonucleotides with high affinity and specificity towards mammosphere cells as enriched stem cells, using MCF-7 as a positive target cell and source of mammosphere cells. Normal breast epithelial, MCF-10A and non-stem like MCF-7sal cells (salinomycin-treated MCF-7 cells) were used as negative target cells. Herein, the MS03 aptamer with good affinity and specificity for mammosphere cells was isolated. Majority of MS03 aptamer-selected cells (63.3%) revealed the $CD44^+/CD24^{-/low}$ phenotype. Therefore, the MS03 aptamer can be used as a breast CSCs biomarker similar to CD44/CD24. The MS03 aptamer may become a favorable molecular probe for breast cancer diagnosis and therapy due to its easy synthesis and non-immunogenic properties [114].

It is demonstrated that the HA binding domain (HABD) is highly conserved in different CD44v [116]. Thus a monothiophosphate-modified aptamer (thioaptamer, TA aptamer) with binding affinity in the range of 180–295 nM for HABD of CD44 was identified which was remarkably more potent that of HA. While the nominated thioaptamer interacted with CD44-positive human ovarian cancer cell lines (SKOV3, IGROV, and A2780) but it was not successful in binding to the CD44-negative NIH3T3 cell line. The site-specific thio substitution at the DNA phosphate backbone initiated a precise and high-affinity binding of thioaptamers to CD44. These aptamers can be regarded as imaging or targeting agents for cancer treatment [115]. Subramanian et al. used thioaptamer-based truncated CD44 aptamers named as TA1 and TA6 (24 and 26 nucleotides) against CD44 as a CSCs marker in CD44-positive retinoblastoma (RB) primary cells and MCF7-sphere. Truncated CD44 aptamer exhibited particular binding and higher affinity towards cancer cells [111]. In another research using *in vitro* selection, a DNA aptasensor named as s5 (s5rev) was developed for recognizing a HABD of CD44 with nanomolar affinity and specificity which efficiently prevented the growth of CD44-overexpressed leukemic cancer cells. The selectivity of platform is verified by an irrelevant interaction with low CD44-expressing cells. The selected aptamers open pave the way towards developing new antitumor strategies based on inhibition of the CD44 [5].

Among the described aptamers for CD44, the modified TA aptamer introduced by Somasunderam research group [115] was chosen for

Table 4
QCM biosensors for CD44 detection.

Strategy	Recognition unit	Target	Sample	LOD	LR	Ref
HA-coated MNPs	HA	Leukemia cells	Human plasma	8×10^3 cells mL^{-1}	–	[99]
SMFS based on immobilized HA and CD44	HA	Vascular endothelium	Blood	–	–	[100]
PDA/PEI/HA film-based QCM biosensor	HA	Breast cancer	Buffer	M-231: 300 cell mL^{-1} MCF-7: 10^3 cells mL^{-1}	M-231:1 $\times 10^3$ to 5×10^5 cells mL^{-1} MCF-7: 5×10^3 to 4×10^5 cells mL^{-1}	[96]
Multi-analyte QCM cytosensor using signal recovery strategy	FA, HA, EGF	Breast cancer	Buffer	5×10^3 cells	3×10^4 to 10^6 cells	[101]
LbL film by using PLL and different size of crosslinked HA	HA	CD44	Buffer	–	–	[102]

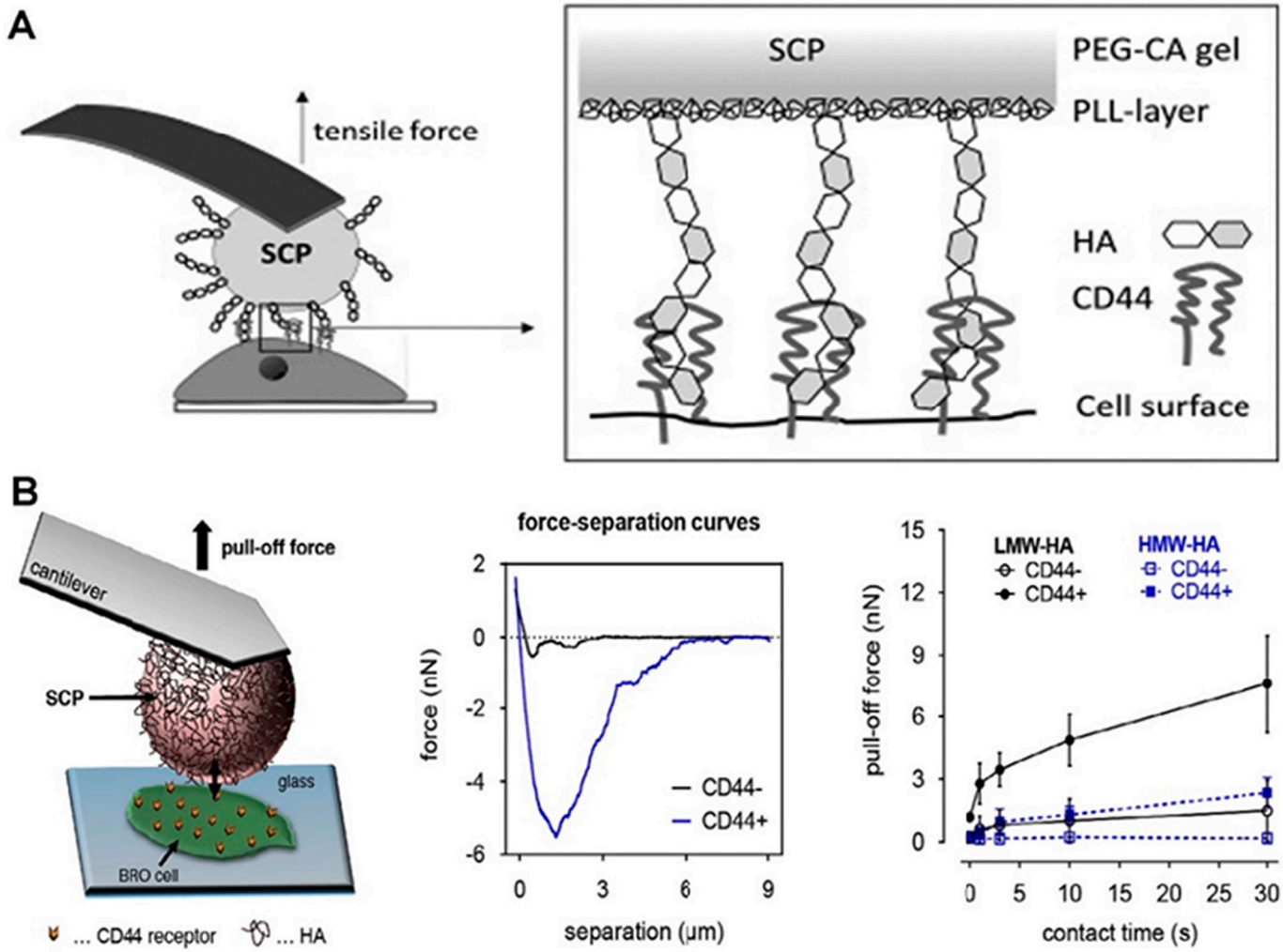

Fig. 12. A) The SCP-AFM technique for the assessment of HA/CD44 interaction with cells; B) The quantification of CD44-HA interaction *via* SCPs approach and typical force-deformation graph of LMW-HA modified SCPs on $CD44^{-}$ (black) and $CD44^{+}$(blue) melanoma cells at 30 s. Reprinted with permission from [103,104]. (For interpretation of the references to color in this figure legend, the reader is referred to the web version of this article.)

Table 5
The presented aptamers for detection of CD44 isoforms.

Selected aptamer	Recognition motif	Target	Aptamer sequence (5′ to 3′)	Ref
Apt1 with 2'-F-pyrimidines	RNA aptamer	CD44-expressed breast cancer	GGGAUGGAUCCAAGCUUACUGGCAUCUGG AUUUGCGCGUGCCAGAAUAAAGAGUAUAACGU GUGAAUGGGAAGCUUCGAUAGGAAUUCGG	[112]
Apt#4 and Apt#7	DNA aptamer	CD44v10	Apt#4: GGGAGACAAGAATAAACGCAACTCCCAGCCCCT CACGTCAGCCCGCTTCGACAGGAGGCTCACAACAGGC Apt#7: GGGAGACAAGAATAAACGCAACCGCGAACCCCC CCCCTTAATGTCATTCGACAGGAGGCTCACAACAGGC	[113]
MS03 aptamer	DNA aptamer	Mammosphere cells	GCATGGGGTTTCGGCGTTTCGT CTATCTTGTTTCTGTTAGCGTCT	[114]
Thioaptamers	DNA aptamer	CD44's HABD	SH-GAGATTCATCACGCGCATAGTC CCAAGGCCTGCAAGGGAACCAAGGA CACAGCGACTATGCGATGATGTCTTC	[115]
Truncated aptamers TA1 and TA6	DNA aptamer	CD44	TA1: CCAAGGCCTGCAAGGGAACCAAGG TA6: GGACGGTGTTAAACGAAAGGGGACGACC	[111]
s5 (s5rev)	DNA aptamer	HABD of CD44	ACCGGGCGTACACCGTCGCGGCACA TGTCTGAATGCGTTTAGTCTCTGTG	[5]

designing aptasensors. In another work, tetramethyl-6-carboxy-rhodamine (TAMRA)-tagged CD44 aptamers were conjugated with GO/AuNPs (GO/AuNPs–TAMRA-Apt) which could specifically determine 1×10^{1} to 1×10^{7} CFU/mL CD44-positive cancer cells with a LOD of 1×10^{1} CFU/mL (Fig. 13A). After hybridization between aptamer and CD44, the fluorescence intensity of TAMRA was induced *via* FRET phenomenon [117]. In a new study, a facile, label-free EIS aptasensor was constructed for serum CD44 determination using a TA aptamer

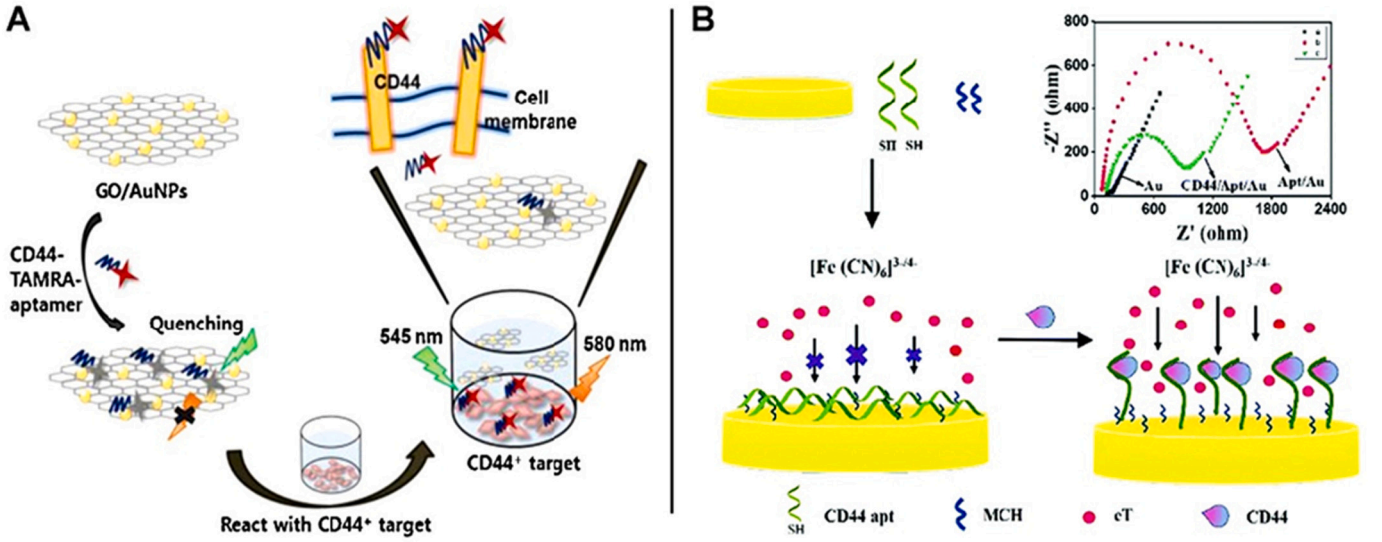

Fig. 13. A) Schematic representation of GO/AuNPs sensing-based CD44-positive cancer cell detection; B) An electrochemical impedance aptasensor for CD44 detection. Reproduced with permission from [117,118].

(CD44 thioaptamer) which was immobilized on Au electrodes. When the target was presented, CD44 was conjugated to the immobilized aptamer resulting in the aptamer structure change, which facilitated the transmission of $[Fe(CN)_6]^{3-/4-}$ through the electrode and the reduction of the impedance of aptasensor (Fig. 13B). The reduced degree of the impedance had a suitable LR for CD44 concentration in the range of 0.1–1000 ng mL^{-1} with a LOD of 0.087 ng mL^{-1} [118].

There is much work to be done to declare the CD44 aptasensors as a valid approach for the POC diagnosis. The CD44 aptamers capable of identifying CD44 in real-case sample and modified against nuclease degradation can probably be nominated for *in vivo* study or preclinical trial phase. Moreover, the degradation, cross-reactivity, interaction with intracellular target, limited metabolism, and clearance of aptamers in biological conditions should be considered [119].

In the present review, we comprehensively discussed the details of a diverse structural design and the performance of existing optical, electrochemical, and QCM-based CD44 biosensors. Tables 1-4 reports a comparison between the methodologies and applications of these biosensing platforms for CD44 detection. The discrepancies in the methodologies might be attributed to a variety of factors that influenced the applicability of the biosensors. The nature of sample (buffer/serum), the recognition motif, framework arrangement, and measurement techniques are among factors to be considered. Individually tweaking these parameters or employing nanomaterials may be able to ameliorate the function of these biosensing scaffolds. Table 6 shows the common advantages and disadvantages of CD44 biosensors approaches.

Table 6
Advantages and disadvantages of optical, electrochemical, and QCM-based biosensors used for the CD44 detection.

Platform	Advantages	Limitations	Ref.
Optical biosensor	Real-time biosensing and quantitative measurements Straightforward and label-free recognition No demand for amplification and sophisticated apparatus Naked-eye readout in colorimetric-based assays Numerous promising utilization for colorimetric-based assays in portable devices	High production costs Low transferability for fluorescence-based sensing platforms No progress in clinical use Time-intensive assembly	[17,120]
Electrochemical biosensor	Quantitative Utilizable Not requiring high sample/reagent volume	Not validated for clinical application Electrolyte-derived false positive data	[120–122]
Piezoelectric-based biosensor	Wide frequency bandwidth High signal-to-noise ratio Reliable operation Constant sensitivity in a wide temperature range	Some piezoelectric materials need moisture proof measures Poor output of DC response	[123,124]

7. Conclusions and future perspectives

Currently, biosensors have become the interesting choice for an accurate, rapid and single or simultaneous recognition of a wide range of cancer biomarkers like CD44 due to their unique features, including high specificity, sensitivity, and stability under different conditions. Another aspect of biosensor-based methods is their optimization from design to application. The improvement of the specificity of the HA and Apt_{CD44} to CD44 along with the modification of the sensor surface by multiple recognition elements can overcome the simultaneous detection concern in real samples. The evidence suggests that employing biomarker panels with "high predictive value" can increase the accuracy of cancer diagnosis using a biosensing design. As a suggestion, survivin (Sur) and Sur mRNA, both of which are identified in all cancer cells, can be combined with CD44 in a single platform to enhance reliability of diagnosis [125,126].

Over recent years, the incorporation of NPs with biosensing platforms as nanobiosensors, has received considerable attention for enhancement of the sensitivity and specificity of biosensors. NPs have large surface/volume ratio improving the efficiency of target interactions, thus nano-biosensors showed low detection limit, which would promise for a new era for accurate diagnosis of different cancers. However, another challenge for NPs is related to their bio-safety and protein corona under *in vivo* conditions, which can affect outcome of CD44-biosensing nanosensors. Most CD44 biosensors reported in previous studies, have been employed *in vitro* while only few studies have been performed for *in vivo* imaging of cancer cells based on CD44 as targeting agents. In one such a work, HA-modified magnetic

nanoclusters (HA-MNCs) could detect the CD44-positive breast cancer cells in tumorized mice model using MRI [127].

To date, there has been no report on clinical application of CD44 biosensors. Given the progress of on-chip and microfluidic-based devices in clinical diagnostics, the-miniaturized nanosensors can be designed and developed as new versatile advanced sensing platforms for the future biomarker-based cancer diagnosis and therapy.

Abbreviations

AuNPs	gold nanoparticles
AFM	atomic force microscopy
ALDH1	aldehyde dehydrogenase 1
AgNPs	silver nanoparticles
AuNRs	gold nanorods
AOTF	acousto-optic tunable filter
BSA	bovine serum albumin
CHI	chitosan
CSCs	cancer stem cells
CCP	cationic conjugated polymer
CD44	Cluster of differentiation 44
CC	chronocoulometry
CL	chemiluminescence
CD44BP	CD44 binding peptide
CNDs	carbon nanodots
CB[8]	cucurbit[*8*]uril
DPV	differential pulse voltammetry
DTDC	3,3-diethylthiadicarbocyanine iodide
DBCO	dibenzocyclooctyne
ECL	electrochemiluminescence
ELISA	enzyme-linked immunosorbent assay
ECM	extracellular matrix
EIS	electrochemical impedance spectroscopy
EGFR	epidermal growth factor receptor
EpCAM	Epithelial cell adhesion molecule
FePc	iron phthalocyanine
FA	folic acid
FRET	Förster resonance energy transfer
FP	Fluorescence polarization
GAGs	glycosaminoglycans
GO	graphene oxide
Gd	gadolinium
HA	hyaluronic acid
HACE	HA-ceramide
ITO	indium tin oxide
IGF-1	Insulin-like growth factor 1
LYVE-1	lymphatic vessel endocytic receptor
LOD	limit of detection
LR	linear range
LSPR	localized-SPR
MGITC	Malachite green isothiocyanate
MWCNTs	multi-walled carbon nanotubes
MSCs	mesenchymal stem cells
MGIP	magnetic glycosyl-imprinted microspheres
MBs	magnetic beads
MNFs	multifunctional nanofibers
MRI	magnetic resonance imaging
MLPA	multiplex ligation-dependent probe amplification
NMs	Nanomaterials
NIRF	near-infrared fluorescence
NSOM	near-field optical microscopy
NIR	near-infrared range
NPs	nanoparticles
PDPP	polyvalent-directed peptide polymer
PATP	*p*-aminobenzoic acid
PEI	polyethylenimine
PEC	photoelectrochemical
PCM	plasmon coupling microscopy
PEG	polyethylene glycol
POC	point-of-care
PDDA	poly(diallyldimethylammonium chloride)
QCM	quartz crystal microbalance
QD	quantum dot
RB	retinoblastoma
RBITC	Rhodamine B isothiocyanate
RHAMM	receptor for HA-mediated motility
R_{ct}	charge transfer resistance
SAW	surface acoustic wave
SCPs	soft colloidal probes
S/N	signal-to-noise
SELEX	Systematic Evolution of Ligands by Exponential Enrichment
SERS	Surface enhanced Raman spectroscopy
CTC	Circulating tumor cell
TAMRA	tetramethyl-6-carboxy-rhodamine
TMB	tetramethylbenzidine
TGFBRII	TGFβ receptor type II
TCPS	tissue culture polystyrene
UCNPs	Upconversion nanoparticles
ZnCQDs	zinc-coadsorbed carbon-QD

CRediT authorship contribution statement

Youkabed Kazem, **Rahim Nosrati**, and **Sadegh Dehghani:** Roles/Writing - original draft; Software. Seyed **Mohammad Taghdisi**, **Khalil Abnous**, **Mona Alibolandi**, and **Mohammad Ramezani**: Supervision; Validation; Writing - Review & Editing.

Declaration of competing interest

The authors declare that they have no known competing financial interests or personal relationships that could have appeared to influence the work reported in this paper.

Acknowledgments

The authors acknowledge the financial support from Mashhad University of Medical Sciences (MUMS), Mashhad, Iran.

References

[1] Z. Fattahi, A.Y. Khosroushahi, M. Hasanzadeh, Recent progress on developing of plasmon biosensing of tumor biomarkers: efficient method towards early stage recognition of cancer, Biomed. Pharmacother. 132 (2020), 110850.
[2] H. Sung J. Ferlay R.L. Siegel M. Laversanne I. Soerjomataram A. Jemal F. Bray n. d. Global cancer statistics 2020: GLOBOCAN estimates of incidence and mortality worldwide for 36 cancers in 185 countries, CA Cancer J. Clin. n/a (n/a).
[3] A. Florea, Z. Taleat, C. Cristea, M. Mazloum-Ardakani, R. Săndulescu, Label free MUC1 aptasensors based on electrodeposition of gold nanoparticles on screen printed electrodes, Electrochem. Commun. 33 (2013) 127–130.
[4] E. Solhi, M. Hasanzadeh, Critical role of biosensing on the efficient monitoring of cancer proteins/biomarkers using label-free aptamer based bioassay, Biomed. Pharmacother. 132 (2020), 110849.
[5] A. Pęcak, Ł. Skalniak, K. Pels, M. Książek, M. Madej, D. Krzemień, S. Malicki, B. Władyka, A. Dubin, T.A. Holak, Anti-CD44 DNA aptamers selectively target cancer cells, Nucleic Acid Ther. 30 (5) (2020) 289–298.
[6] M.N. Mishra, V. Chandavarkar, R. Sharma, D. Bhargava, Structure, function and role of CD44 in neoplasia, J. Oral Maxillofac. Pathol. 23 (2) (2019) 267–272.
[7] S.Y. Lee, M.S. Kang, W.Y. Jeong, D.-W. Han, K.S. Kim, Hyaluronic acid-based theranostic nanomedicines for targeted cancer therapy, Cancers (Basel) 12 (4) (2020) 940.
[8] Y. Qiu, B. Zhou, X. Yang, D. Long, Y. Hao, P. Yang, Novel single-cell analysis platform based on a solid-state zinc-coadsorbed carbon quantum dots electrochemiluminescence probe for the evaluation of CD44 expression on breast cancer cells, ACS Appl. Mater. Interfaces 9 (20) (2017) 16848–16856.
[9] Z.A. Nima, M. Mahmood, Y. Xu, T. Mustafa, F. Watanabe, D.A. Nedosekin, M. A. Juratli, T. Fahmi, E.I. Galanzha, J.P. Nolan, Circulating tumor cell identification by functionalized silver-gold nanorods with multicolor, super-enhanced SERS and photothermal resonances, Sci. Rep. 4 (1) (2014) 1–8.

[10] Z. Yu, T.G. Pestell, M.P. Lisanti, R.G. Pestell, Cancer stem cells, Int. J. Biochem. Cell Biol. 44 (12) (2012) 2144–2151.
[11] S. Chenaghlou, A. Khataee, R. Jalili, M.-R. Rashidi, B. Khalilzadeh, S.W. Joo, Gold nanostar-enhanced electrochemiluminescence immunosensor for highly sensitive detection of cancer stem cells using CD133 membrane biomarker, Bioelectrochemistry 137 (2020), 107633.
[12] A. Reithmeier, Tartrate-resistant Acid Phosphatase/ACP5 as a Driver of Cancer: Dissection of Its Oncogenic Mechanisms and Identification of Small Molecule Inhibitors, Inst för laboratoriemedicin/Dept of Laboratory Medicine, 2017.
[13] R. Thapa, G.D. Wilson, The importance of CD44 as a stem cell biomarker and therapeutic target in cancer, Stem Cells Int. 2016 (2016) 2087204.
[14] Z. Wang, Y. Tang, L. Xie, A. Huang, C. Xue, Z. Gu, K. Wang, S. Zong, The prognostic and clinical value of CD44 in colorectal cancer: a meta-analysis, Front. Oncol. 9 (2019) 309.
[15] S. Shinohara, T. Hanagiri, A. Taira, M. Takenaka, S. Oka, Y. Chikaishi, H. Uramoto, T. So, S. Yamada, F. Tanaka, Immunohistochemical expression and serum levels of CD44 as prognostic indicators in patients with non-small cell lung cancer, Oncology 90 (6) (2016) 327–338.
[16] J. Kirsch, C. Siltanen, Q. Zhou, A. Revzin, A. Simonian, Biosensor technology: recent advances in threat agent detection and medicine, Chem. Soc. Rev. 42 (22) (2013) 8733–8768.
[17] V. Perumal, U. Hashim, Advances in biosensors: principle, architecture and applications, J. Appl. Biomed. 12 (1) (2014) 1–15.
[18] A.A. Nayl, A.I. Abd-Elhamid, A.Y. El-Moghazy, M. Hussin, M.A. Abu-Saied, A. A. El-Shanshory, H.M.A. Soliman, The nanomaterials and recent progress in biosensing systems: a review, Trends Environ. Anal. Chem. 26 (2020), e00087.
[19] B. Purohit, P.R. Vernekar, N.P. Shetti, P. Chandra, Biosensor nanoengineering: design, operation, and implementation for biomolecular analysis, Sens. Int. 1 (2020), 100040.
[20] C. Chen, J. Wang, Optical biosensors: an exhaustive and comprehensive review, Analyst 145 (5) (2020) 1605–1628.
[21] I. Obodovskiy, Chapter 12 - luminescence, in: I. Obodovskiy (Ed.), Radiation, Elsevier, 2019, pp. 207–220.
[22] L. Bouffier, N. Sojic, Introduction and overview of electrogenerated chemiluminescence, in: Analytical Electrogenerated Chemiluminescence: From Fundamentals to Bioassays, 2019, pp. 1–28.
[23] A. Roda, M. Mirasoli, E. Michelini, M. Di Fusco, M. Zangheri, L. Cevenini, B. Roda, P. Simoni, Progress in chemical luminescence-based biosensors: a critical review, Biosens. Bioelectron. 76 (2016) 164–179.
[24] M. Mirasoli, M. Guardigli, E. Michelini, A. Roda, Recent advancements in chemical luminescence-based lab-on-chip and microfluidic platforms for bioanalysis, J. Pharm. Biomed. Anal. 87 (2014) 36–52.
[25] J. Chen, Y. Pei, Z. Chen, J. Cai, Quantum dot labeling based on near-field optical imaging of CD44 molecules, Micron 41 (3) (2010) 198–202.
[26] A. De Thomaz, D. Almeida, V. Pelegati, H. Carvalho, C. Cesar, Measurement of the hydrodynamic radius of quantum dots by fluorescence correlation spectroscopy excluding blinking, J. Phys. Chem. B 119 (11) (2015) 4294–4299.
[27] P. Zuo, X. Lu, Z. Sun, Y. Guo, H. He, A review on syntheses, properties, characterization and bioanalytical applications of fluorescent carbon dots, Microchim. Acta 183 (2) (2016) 519–542.
[28] M.J. Molaei, Carbon quantum dots and their biomedical and therapeutic applications: a review, RSC Adv. 9 (12) (2019) 6460–6481.
[29] Z. Wang, J. Yu, R. Gui, H. Jin, Y. Xia, Carbon nanomaterials-based electrochemical aptasensors, Biosens. Bioelectron. 79 (2016) 136–149.
[30] J. Luo, L.J. Cote, V.C. Tung, A.T.L. Tan, P.E. Goins, J. Wu, J. Huang, Graphene oxide nanocolloids, J. Am. Chem. Soc. 132 (50) (2010) 17667–17669.
[31] K. Muazim, Z. Hussain, Graphene oxide — a platform towards theranostics, Mater. Sci. Eng. C 76 (2017) 1274–1288.
[32] J. Ping, Y. Zhou, Y. Wu, V. Papper, S. Boujday, R.S. Marks, T.W.J. Steele, Recent advances in aptasensors based on graphene and graphene-like nanomaterials, Biosens. Bioelectron. 64 (2015) 373–385.
[33] J.C. Pickup, F. Hussain, N.D. Evans, O.J. Rolinski, D.J.S. Birch, Fluorescence-based glucose sensors, Biosens. Bioelectron. 20 (12) (2005) 2555–2565.
[34] X. Ou, S. Zhan, C. Sun, Y. Cheng, X. Wang, B. Liu, T. Zhai, X. Lou, F. Xia, Simultaneous detection of telomerase and miRNA with graphene oxide-based fluorescent aptasensor in living cells and tissue samples, Biosens. Bioelectron. 124 (2019) 199–204.
[35] X. Ma, Z. Jiang, J. Li, An electrochemiluminescence sensor of magnetic glycosyl-imprinted microspheres based on multi-probe signal amplification for CD44v6 determination, Sensors Actuators B Chem. 333 (2021), 129562.
[36] B. Babamiri, D. Bahari, A. Salimi, Highly sensitive bioaffinity electrochemiluminescence sensors: recent advances and future directions, Biosens. Bioelectron. 142 (2019), 111530.
[37] B. Hötzer, I.L. Medintz, N. Hildebrandt, Fluorescence in nanobiotechnology: sophisticated fluorophores for novel applications, Small 8 (15) (2012) 2297–2326.
[38] M. Strianese, M. Staiano, G. Ruggiero, T. Labella, C. Pellecchia, S. D'Auria, Fluorescence-based biosensors, in: Spectroscopic Methods of Analysis, Springer, 2012, pp. 193–216.
[39] K. Girigoswami, N. Akhtar, Nanobiosensors and fluorescence based biosensors: an overview, Int. J. Nano Dimens 10 (1) (2019) 1–17.
[40] Y. Huang, X. Yao, R. Zhang, L. Ouyang, R. Jiang, X. Liu, C. Song, G. Zhang, Q. Fan, L. Wang, Cationic conjugated polymer/fluoresceinamine-hyaluronan complex for sensitive fluorescence detection of CD44 and tumor-targeted cell imaging, ACS Appl. Mater. Interfaces 6 (21) (2014) 19144–19153.
[41] A.M. Carvalho, D.S. da Costa, P.M. Paulo, R.L. Reis, I. Pashkuleva, Co-localization and crosstalk between CD44 and RHAMM depend on hyaluronan presentation, Acta Biomater. 119 (2020) 114–124.
[42] C. Berney, G. Danuser, FRET or no FRET: a quantitative comparison, Biophys. J. 84 (6) (2003) 3992–4010.
[43] J.A. Sánchez, O. Henry, H. Joda, B.W. Solnestam, L. Kvastad, E. Johansson, P. Akan, J. Lundeberg, N. Lladach, D. Ramakrishnan, Multiplex PCB-based electrochemical detection of cancer biomarkers using MLPA-barcode approach, Biosensors Bioelectron. 82 (2016) 224–232.
[44] J.-H. Cho, S.-C. Lee, N.-R. Ha, S.-J. Lee, M.-Y. Yoon, A novel peptide-based recognition probe for the sensitive detection of CD44 on breast cancer stem cells, Mol. Cell. Probes 29 (6) (2015) 492–499.
[45] Y. Shim, J.M. Song, Spectral overlap-free quantum dot-based determination of benzo [a] pyrene-induced cancer stem cells by concurrent monitoring of CD44, CD24 and aldehyde dehydrogenase 1, Chem. Commun. 51 (11) (2015) 2118–2121.
[46] T. Jia, C. Fu, C. Huang, H. Yang, N. Jia, Highly sensitive naphthalimide-based fluorescence polarization probe for detecting cancer cells, ACS Appl. Mater. Interfaces 7 (18) (2015) 10013–10021.
[47] H. Sun, R.V. Benjaminsen, K. Almdal, T.L. Andresen, Hyaluronic acid immobilized polyacrylamide nanoparticle sensors for CD44 receptor targeting and pH measurement in cells, Bioconj. Chem. 23 (11) (2012) 2247–2255.
[48] H.-J. Cho, H.Y. Yoon, H. Koo, S.-H. Ko, J.-S. Shim, J.-H. Cho, J.H. Park, K. Kim, I. C. Kwon, D.-D. Kim, Hyaluronic acid-ceramide-based optical/MR dual imaging nanoprobe for cancer diagnosis, J. Control. Release 162 (1) (2012) 111–118.
[49] F. Du, X. Zhao, W. Lu, Z. Guo, S. Shuang, C. Dong, Dual-ligand functionalized carbon nanodots as green fluorescent nanosensors for cellular dual receptor-mediated targeted imaging, Analyst 144 (22) (2019) 6729–6735.
[50] Y. Feng, Y. Su, R. Liu, Y. Lv, Engineering activatable nanoprobes based on time-resolved luminescence for chemo/biosensing, TrACTrends Anal. Chem. 140 (2021), 116283.
[51] Y. Song, W. Wei, X. Qu, Colorimetric biosensing using smart materials, Adv. Mater. 23 (37) (2011) 4215–4236.
[52] H. Aldewachi, T. Chalati, M. Woodroofe, N. Bricklebank, B. Sharrack, P. Gardiner, Gold nanoparticle-based colorimetric biosensors, Nanoscale 10 (1) (2018) 18–33.
[53] M.H. Jeoung, T.-K. Kim, H. Shim, S. Lee, Development of a sandwich enzyme-linked immunosorbent assay for the detection of CD44v3 using exon v3- and v6-specific monoclonal antibody pairs, J. Immunol. Methods 436 (2016) 22–28.
[54] Ç. Kip, E. Akbay, B. Gökçal, B.O. Savaş, M.A. Onur, A. Tuncel, Colorimetric determination of tumor cells via peroxidase-like activity of a cell internalizable nanozyme: hyaluronic acid attached-silica microspheres containing accessible magnetite nanoparticles, Colloids Surf. Physicochem. Eng. Aspects 598 (2020), 124812.
[55] C. Solier, H. Langen, Antibody-based proteomics and biomarker research—current status and limitations, Proteomics 14 (6) (2014) 774–783.
[56] G.A. Posthuma-Trumpie, J. Korf, A. van Amerongen, Lateral flow (immuno) assay: its strengths, weaknesses, opportunities and threats. A literature survey, Anal. Bioanal. Chem. 393 (2) (2009) 569–582.
[57] N. Ajdari, C. Vyas, S.L. Bogan, B.A. Lwaleed, B.G. Cousins, Gold nanoparticle interactions in human blood: a model evaluation, Nanomed. Nanotechnol. Biol. Med. 13 (4) (2017) 1531–1542.
[58] S.V. Hamidi, J. Perreault, Simple rolling circle amplification colorimetric assay based on pH for target DNA detection, Talanta 201 (2019) 419–425.
[59] M. Mahmoudpour, J.E.N. Dolatabadi, M. Torbati, A. Homayouni-Rad, Nanomaterials based surface plasmon resonance signal enhancement for detection of environmental pollutions, Biosensors Bioelectron. 127 (2019) 72–84.
[60] S. Zhan, X. Lou, P. Zhou, F. Xia, Sandwich assays based on SPR, SERS, GMR, QCM, microcantilever, SAW, and RRS techniques for protein detection, in: Biosensors Based on Sandwich Assays, Springer, 2018, pp. 69–91.
[61] A. De La Escosura-Muniz, C. Parolo, A. Merkoçi, Immunosensing using nanoparticles, Mater. Today 13 (7–8) (2010) 24–34.
[62] H.B. Seo, M.B. Gu, Aptamer-based sandwich-type biosensors, J. Biol. Eng. 11 (1) (2017) 11.
[63] X. Yu, J. Wang, A. Feizpour, B.R.M. Reinhard, Illuminating the lateral organization of cell-surface CD24 and CD44 through plasmon coupling between Au nanoparticle immunolabels, Anal. Chem. 85 (3) (2013) 1290–1294.
[64] X. Liu, R. Huang, R. Su, W. Qi, L. Wang, Z. He, Grafting hyaluronic acid onto gold surface to achieve low protein fouling in surface plasmon resonance biosensors, ACS Appl. Mater. Interfaces 6 (15) (2014) 13034–13042.
[65] P.R. Rauta, P.M. Hallur, A. Chaubey, Gold nanoparticle-based rapid detection and isolation of cells using ligand-receptor chemistry, Sci. Rep. 8 (1) (2018) 1–13.
[66] J. Langer, D. Jimenez de Aberasturi, J. Aizpurua, R.A. Alvarez-Puebla, B. Auguié, J.J. Baumberg, G.C. Bazan, S.E. Bell, A. Boisen, A.G. Brolo, Present and future of surface-enhanced Raman scattering, ACS Nano 14 (1) (2019) 28–117.
[67] A.I. Pérez-Jiménez, D. Lyu, Z. Lu, G. Liu, B. Ren, Surface-enhanced Raman spectroscopy: benefits, trade-offs and future developments, Chem. Sci. 11 (18) (2020) 4563–4577.
[68] G. Demirel, H. Usta, M. Yilmaz, M. Celik, H.A. Alidagi, F. Buyukserin, Surface-enhanced Raman spectroscopy (SERS): an adventure from plasmonic metals to organic semiconductors as SERS platforms, J. Mater. Chem. C 6 (20) (2018) 5314–5335.
[69] U. Dinish, G. Balasundaram, Y.-T. Chang, M. Olivo, Actively targeted in vivo multiplex detection of intrinsic cancer biomarkers using biocompatible SERS nanotags, Sci. Rep. 4 (1) (2014) 1–7.
[70] E. Petryayeva, U.J. Krull, Localized surface plasmon resonance: nanostructures, bioassays and biosensing—a review, Anal. Chim. Acta 706 (1) (2011) 8–24.

[71] T. Xu, Z. Geng, Strategies to improve performances of LSPR biosensing: structure, materials, and interface modification, Biosensors Bioelectron. 174 (2021), 112850.
[72] K. Lee, V.P. Drachev, J. Irudayaraj, DNA−Gold nanoparticle reversible networks grown on cell surface marker sites: application in diagnostics, ACS Nano 5 (3) (2011) 2109–2117.
[73] C. Yu, H. Nakshatri, J. Irudayaraj, Identity profiling of cell surface markers by multiplex gold nanorod probes, Nano Lett. 7 (8) (2007) 2300–2306.
[74] N. Choi, H. Dang, A. Das, M.S. Sim, I.Y. Chung, J. Choo, SERS biosensors for ultrasensitive detection of multiple biomarkers expressed in cancer cells, Biosensors Bioelectron. 164 (2020), 112326.
[75] D. Grieshaber, R. MacKenzie, J. Vörös, E. Reimhult, Electrochemical biosensors-sensor principles and architectures, Sensors 8 (3) (2008) 1400–1458.
[76] B. Wang, U. Akiba, J.-I. Anzai, Recent Progress in nanomaterial-based electrochemical biosensors for cancer biomarkers: a review, Molecules 22 (7) (2017) 1048.
[77] X. Luo, J.J. Davis, Electrical biosensors and the label free detection of protein disease biomarkers, Chem. Soc. Rev. 42 (13) (2013) 5944–5962.
[78] M. Oguzhan Caglayan, Electrochemical aptasensors for early cancer diagnosis: a review, Curr. Anal. Chem. 13 (1) (2017) 18–30.
[79] F. Cui, Z. Zhou, H.S. Zhou, Measurement and analysis of cancer biomarkers based on electrochemical biosensors, J. Electrochem. Soc. 167 (3) (2019), 037525.
[80] S. Eissa, R. Chinnappan, M. Zourob, Label-free impedimetric immunosensors for liver cancer stem cells, Procedia Technol. 27 (2017) 287–289.
[81] S. Eissa, R. Chinnappan, M. Zourob, Ultrasensitive label-free electrochemical immunosensors for multiple cell surface biomarkers on liver cancer stem cells, Electroanalysis 29 (8) (2017) 1994–2000.
[82] B. Fan, Q. Fan, M. Cui, T. Wu, J. Wang, H. Ma, Q. Wei, Photoelectrochemical biosensor for sensitive detection of soluble CD44 based on the facile construction of a poly (ethylene glycol)/hyaluronic acid hybrid antifouling interface, ACS Appl. Mater. Interfaces 11 (27) (2019) 24764–24770.
[83] J. Zhao, Y. Tang, Y. Cao, T. Chen, X. Chen, X. Mao, Y. Yin, G. Chen, Amplified electrochemical detection of surface biomarker in breast cancer stem cell using self-assembled supramolecular nanocomposites, Electrochim. Acta 283 (2018) 1072–1078.
[84] M. Liu, Y. Xu, C. Huang, T. Jia, X. Zhang, D.-P. Yang, N. Jia, Hyaluronic acid-grafted three-dimensional MWCNT array as biosensing interface for chronocoulometric detection and fluorometric imaging of CD44-overexpressing cancer cells, Microchim. Acta 185 (7) (2018) 1–8.
[85] R. Zhang, C. Rejeeth, W. Xu, C. Zhu, X. Liu, J. Wan, M. Jiang, K. Qian, Label-free electrochemical sensor for cd44 by ligand-protein interaction, Anal. Chem. 91 (11) (2019) 7078–7085.
[86] S.L. Moura, C.G. Martín, M. Martí, M.I. Pividori, Electrochemical immunosensing of nanovesicles as biomarkers for breast cancer, Biosensors Bioelectron. 150 (2020), 111882.
[87] C. Rejeeth, X. Pang, R. Zhang, W. Xu, X. Sun, B. Liu, J. Lou, J. Wan, H. Gu, W. Yan, Extraction, detection, and profiling of serum biomarkers using designed Fe 3 O 4@ SiO 2@ HA core–shell particles, Nano Res. 11 (1) (2018) 68–79.
[88] J.B.M. Rocha Neto, A.C. Soares, R.A. Bataglioli, O. Carr, C.A.R. Costa, O. N. Oliveira, M.M. Beppu, H.F. Carvalho, Polysaccharide multilayer films in sensors for detecting prostate tumor cells based on hyaluronan-CD44 interactions, Cells 9 (6) (2020) 1563.
[89] Z. Wang, J. Li, W. Tu, H. Wang, Z. Wang, Z. Dai, Formation of a photoelectrochemical Z-scheme structure with inorganic/organic hybrid materials for evaluation of receptor protein expression on the membrane of cancer cells, ACS Appl. Mater. Interfaces 12 (24) (2020) 26905–26913.
[90] R.A. Soomro, S. Jawaid, N.H. Kalawar, M. Tunesi, S. Karakuş, A. Kilislioğlu, M. Willander, In-situ engineered MXene-TiO2/BiVO4 hybrid as an efficient photoelectrochemical platform for sensitive detection of soluble CD44 proteins, Biosensors Bioelectron. 166 (2020), 112439.
[91] Y. Tang, Y. Dai, X. Huang, L. Li, B. Han, Y. Cao, J. Zhao, Self-assembling peptide-based multifunctional nanofibers for electrochemical identification of breast cancer stem-like cells, Anal. Chem. 91 (12) (2019) 7531–7537.
[92] Y. Wang, L. Dong, J. Zhao, M. Jalalah, M. Al-Assiri, F.A. Harraz, Y. Cao, Proximity-constructed bifunctional DNA probes for identification of stem-like biomarker in breast cancer, Sensors Actuators B Chem. 328 (2020), 129044.
[93] Y. Zhou, Y. Wan, M. Yu, X. Yuan, C. Zhang, Hyaluronic acid-based label-free electrochemical impedance analysis for cancer cell quantification and CD44 expression, Microchem. J. 160 (2021), 105622.
[94] P. Jandas, J. Luo, A. Quan, C. Li, C. Fu, Y. Fu, Graphene oxide-au nano particle coated quartz crystal microbalance biosensor for the real time analysis of carcinoembryonic antigen, RSC Adv. 10 (7) (2020) 4118–4128.
[95] M. Pohanka, Overview of piezoelectric biosensors, immunosensors and DNA sensors and their applications, Materials 11 (3) (2018) 448.
[96] X. Yang, R. Zhou, Y. Hao, P. Yang, A CD44-biosensor for evaluating metastatic potential of breast cancer cells based on quartz crystal microbalance, Sci. Bull. 62 (13) (2017) 923–930.
[97] S. Tombelli, M. Minunni, M. Mascini, Piezoelectric biosensors: strategies for coupling nucleic acids to piezoelectric devices, Methods 37 (1) (2005) 48–56.
[98] M.A. Cooper, Label-free screening of bio-molecular interactions, Anal. Bioanal. Chem. 377 (5) (2003) 834–842.
[99] Y. Zhou, Q. Xie, Hyaluronic acid-coated magnetic nanoparticles-based selective collection and detection of leukemia cells with quartz crystal microbalance, Sensors Actuators B Chem. 223 (2016) 9–14.
[100] F. Bano, S. Banerji, M. Howarth, D.G. Jackson, R.P. Richter, A single molecule assay to probe monovalent and multivalent bonds between hyaluronan and its key leukocyte receptor CD44 under force, Sci. Rep. 6 (1) (2016) 1–14.
[101] B. Zhou, Y. Hao, D. Long, P. Yang, Real-time quartz crystal microbalance cytosensor based on a signal recovery strategy for in-situ and continuous monitoring of multiple cell membrane glycoproteins, Biosens. Bioelectron. 111 (2018) 90–96.
[102] S. Amorim, I. Pashkuleva, C.A. Reis, R.L. Reis, R.A. Pires, Tunable layer-by-layer films containing hyaluronic acid and their interactions with CD44, J. Mater. Chem. B 8 (17) (2020) 3880–3885.
[103] S. Martin, H. Wang, T. Rathke, U. Anderegg, S. Möller, M. Schnabelrauch, T. Pompe, S. Schmidt, Polymer hydrogel particles as biocompatible AFM probes to study CD44/hyaluronic acid interactions on cells, Polymer 102 (2016) 342–349.
[104] J. Sapudom, F. Ullm, S. Martin, L. Kalbitzer, J. Naab, S. Möller, M. Schnabelrauch, U. Anderegg, S. Schmidt, T. Pompe, Molecular weight specific impact of soluble and immobilized hyaluronan on CD44 expressing melanoma cells in 3D collagen matrices, Acta Biomater. 50 (2017) 259–270.
[105] A.D. Keefe, S. Pai, A. Ellington, Aptamers as therapeutics, Nat. Rev. Drug Discov. 9 (7) (2010) 537–550.
[106] T. Adachi, Y. Nakamura, Aptamers: a review of their chemical properties and modifications for therapeutic application, Molecules 24 (23) (2019) 4229.
[107] M. Famulok, G. Mayer, Aptamers and SELEX in chemistry & biology, Chem. Biol. 21 (9) (2014) 1055–1058.
[108] D. Ogasawara, N.S. Hachiya, K. Kaneko, K. Sode, K. Ikebukuro, Detection system based on the conformational change in an aptamer and its application to simple bound/free separation, Biosens. Bioelectron. 24 (5) (2009) 1372–1376.
[109] D. Ruiz Ciancio, M.R. Vargas, W.H. Thiel, M.A. Bruno, P.H. Giangrande, M. B. Mestre, Aptamers as diagnostic tools in cancer, Pharmaceuticals (Basel) 11 (3) (2018) 86.
[110] Y.M. Chang, M.J. Donovan, W. Tan, Using aptamers for cancer biomarker discovery, J. Nucleic Acids 2013 (2013).
[111] N. Subramanian, B. Akilandeswari, A. Bhutra, M. Alameen, U. Vetrivel, V. Khetan, R.K. Kanwar, J.R. Kanwar, S. Krishnakumar, Targeting CD44, ABCG2 and CD133 markers using aptamers: in silico analysis of CD133 extracellular domain 2 and its aptamer, RSC Adv. 6 (38) (2016) 32115–32123.
[112] N. Ababneh, W. Alshaer, O. Al-Louzi, A. Mahafzah, M. El-Khateeb, H. Hillaireau, M. Noiray, E. Fattal, S. Ismail, In vitro selection of modified RNA aptamers against CD44 cancer stem cell marker, Nucleic Acid Ther. 23 (6) (2013) 401–407.
[113] J. Iida, R. Clancy, J. Dorchak, R.I. Somiari, S. Somiari, M.L. Cutler, R.J. Mural, C. D. Shriver, DNA aptamers against exon v10 of CD44 inhibit breast cancer cell migration, PLoS One 9 (2) (2014), e88712.
[114] M. Lu, L. Zhou, X. Zheng, Y. Quan, X. Wang, X. Zhou, J. Ren, A novel molecular marker of breast cancer stem cells identified by cell-SELEX method, Cancer Biomark. 15 (2) (2015) 163–170.
[115] A. Somasunderam, V. Thiviyanathan, T. Tanaka, X. Li, M. Neerathilingam, G.L. R. Lokesh, A. Mann, Y. Peng, M. Ferrari, J. Klostergaard, Combinatorial selection of DNA thioaptamers targeted to the HA binding domain of human CD44, Biochemistry 49 (42) (2010) 9106–9112.
[116] P.M. Wolny, S. Banerji, C. Gounou, A.R. Brisson, A.J. Day, D.G. Jackson, R. P. Richter, Analysis of CD44-hyaluronan interactions in an artificial membrane system: insights into the distinct binding properties of high and low molecular weight hyaluronan, J. Biol. Chem. 285 (39) (2010) 30170–30180.
[117] H.Y. Jeong, S.H. Baek, S.-J. Chang, S.A. Cheon, T.J. Park, Robust fluorescence sensing platform for detection of CD44 cells based on graphene oxide/gold nanoparticles, Colloids Surf. B. Biointerfaces 135 (2015) 309–315.
[118] J. Zhou, K. Cheng, X. Chen, R. Yang, M. Lu, L. Ming, Y. Chen, Z. Lin, D. Chen, Determination of soluble CD44 in serum by using a label-free aptamer based electrochemical impedance biosensor, Analyst 145 (2) (2020) 460–465.
[119] A. Lakhin, V. Tarantul, L. Gening, Aptamers: problems, solutions and prospects, Acta Naturae 5 (4 (19)) (2013).
[120] A.A. Jamali, M. Pourhassan-Moghaddam, J.E.N. Dolatabadi, Y. Omidi, Nanomaterials on the road to microRNA detection with optical and electrochemical nanobiosensors, trendsAnal. Chem. 55 (2014) 24–42.
[121] X. Zuo, S. Song, J. Zhang, D. Pan, L. Wang, C. Fan, A target-responsive electrochemical aptamer switch (TREAS) for reagentless detection of nanomolar ATP, J. Am. Chem. Soc. 129 (5) (2007) 1042–1043.
[122] A.A. Saei, J.E.N. Dolatabadi, P. Najafi-Marandi, A. Abhari, M. de la Guardia, Electrochemical biosensors for glucose based on metal nanoparticles, Trends Anal. Chem. 42 (2013) 216–227.
[123] S. Song, Y. Hou, M. Guo, L. Wang, X. Tong, J. Wu, An investigation on the aggregate-shape embedded piezoelectric sensor for civil infrastructure health monitoring, Constr. Build. Mater. 131 (2017) 57–65.
[124] C.C. Vu, J. Kim, Waterproof, thin, high-performance pressure sensors-hand drawing for underwater wearable applications, Sci. Technol. Adv. Mater. 22 (1) (2021) 718–728.
[125] M. Stobiecka, K. Ratajczak, S. Jakiela, Toward early cancer detection: focus on biosensing systems and biosensors for an anti-apoptotic protein survivin and survivin mRNA, Biosensors Bioelectron. 137 (2019) 58–71.
[126] M. Stobiecka, A. Chalupa, B. Dworakowska, Piezometric biosensors for anti-apoptotic protein surviving based on buried positive-potential barrier and immobilized monoclonal antibodies, Biosens. Bioelectron. 84 (2016) 37–43.
[127] E.-K. Lim, H.-O. Kim, E. Jang, J. Park, K. Lee, J.-S. Suh, Y.-M. Huh, S. Haam, Hyaluronan-modified magnetic nanoclusters for detection of CD44-overexpressing breast cancer by MR imaging, Biomaterials 32 (31) (2011) 7941–7950.